INSTITUTE

FOR

AEROSPACE STUDIES

UNIVERSITY OF TORONTO

EFFECTS OF STRUCTURAL FLEXIBILITY ON A REACTION JET SATELLITE ATTITUDE CONTROL SYSTEM

by

Gunter Malich

December 1975

UTIAS Technical Note No. 199
CN ISSN 0082-5263

EFFECTS OF STRUCTURAL FLEXIBILITY
ON A REACTION JET SATELLITE ATTITUDE CONTROL SYSTEM

by

Gunter Malich

UTIAS Technical Note No. 199
CN ISSN 0082-5263

December, 1975

Acknowledgements

The author is indebted to Dr. P. C. Hughes for suggesting this topic of investigation, and for his continued interest and helpful discussion.

The work described herein was made possible through the financial assistance of the Federal Department of Communications (Communications Research Centre), Contract No. OSR3-0017.

Summary

The performance of a satellite reaction jet attitude control system can be severely degraded by structural flexibility. Using a computer-modelled spacecraft with a pseudo-rate controller, a quantification of the performance loss is presented. Flexibility has been introduced into the simulation in a very general way by reducing elastic interaction to a series of modal frequency and gain parameters. The modelled system has been found to remain stable under all conditions studied, although performance may suffer various degrees of degradation.

TABLE OF CONTENTS

NOTATION

Algebraic	Computer	Definition
DB	DB	Dead-band of controller
H	H	PSR hysteresis
I_f	IFLEX	Inertia of flexible part
I_r	IRIG	Inertia of rigid part
I	ITOT	Total inertia
K_f	KF	PSR feedback gain
K_{jet}	KJET	Thruster torque gain
k_1	K1U	Mode 1 unconstrained gain
K_1	K1C	Mode 1 constrained gain
K_θ	KTHETA	Sensor gain
R	R	PSR controller output
r	-	Thruster duty cycle
T_c	TC	Control torque
T_D	TD	Disturbance torque
T_{net}	TNET	net torque
T_{eff}	-	Effective torque
t	TIME	Real time
t_{on}	TON	Thruster "on-time"
t_{off}	-	Thruster "off-time"
t*	TSTAR	System characteristic period
α	ALPHA	Acceleration
β	BETA	I_f/I_t
ϵ_1	EPS1	Sensor output
ϵ_2	EPS2	PSR feedback error
ϵ_3	EPS3	PSR controller input

NOTATION - Continued

Algebraic	Computer	Definition
θ	TH	Body angle
θ_E	THE	Error angle to sensor
θ_I	THI	Control angle
θ_R	THR	Body angle of rigid part
θ_1	TH1	Body angle of mode 1
ζ	DAMP	Appendage damping factor
τ_f	TAUF	PSR feedback time constant
Φ	PHIC	Ω_1/ω_c
ϕ	PHIU	ω_1/ω_c
ω_c	WN	Control loop natural frequency
Ω_1	W1C	Mode 1 constrained frequency
ω_1	W1U	Mode 1 unconstrained frequency
$\hat{X}$	XN	Nondimensional form of "X"
$\dot{X}$	DX	Time derivative of "X"
X_o	XO	Initial condition of "X"

1. INTRODUCTION

The study of structural flexibility and its effect on control system performance has become of crucial importance in the design of modern space vehicles. This was poignantly brought to light in Explorer I, as previously unknown effects of whip antenna motion led to dynamic instability. A few years later, the success of OGO III was seriously hampered by excessive oscillations created by control system interactions with flexible booms. There are many other examples of space missions being hampered by these problems. The interested reader is directed to Ref. 1 for an outline. Reference 8 also provides an informative overview of flexibility effects on control systems.

Structural flexibility has been, and will probably continue to be, an important area of study. With spacecraft power consumption and sophistication on the increase, antennae and solar arrays tend towards greater prominence. If costly weight penalties are to be avoided, this is bound to result in less appendage rigidity. There are limits to the degree of flexibility which can be tolerated. Excessive appendage motion can feed back into the body of the satellite, and hamper pointing accuracy. Furthermore, the added accelerations created by appendage oscillations are bound to increase the stress and fatigue levels on the spacecraft.

Particular problems can be created for those vehicles with an active control system, such as the previously mentioned OGO III. Active systems incorporate sensors to check satellite attitude and a controller to supply torques to maintain some desired attitude. Excessive motions of the vehicle, as a result of flexibility-induced oscillations, will tend to trigger the attitude control system more often than for a rigid satellite. The control torques applied can produce an added fuel consumption, a degraded control response, and even instability.

Investigating flexibility interactions through ground testing is both costly and dynamically awkward. Structures designed for the weightless state do not lend themselves well to a one-g field. Structural engineers therefore try to design appendages stiff enough so that interaction problems are unlikely to occur. This generally entails arranging for the natural vibration frequencies of the structure to be much higher than the passband of the attitude controller. This results in a trade-off between costly stiffness, and design confidence.

It becomes imperative to estimate the amount of performance lost for a given loss in rigidity. An attempt is made in this Note to contribute towards this estimate. With the aid of a computer model, a simple satellite with a nonlinear attitude control system is simulated. The analysis is arranged so that the ratio of 'flexible' inertia to total inertia can be varied. In this way, dynamic effects are modelled from a fully rigid to a fully flexible satellite. The structural model, in conjunction with the attitude control system model, thus allows an investigation into the interactions of structural flexibility, control performance, and stability.

2. THE GENERAL MODEL

In order to help isolate the effects of flexibility on attitude control, it is desirable to investigate a reasonably simple satellite model.

Though this entails a loss of accuracy for individual spacecraft, results can be of a more general nature.

A diagram demonstrating the vehicle studied is shown in Fig. 1. The model is assumed to possess a symmetric structure, with a central rigid body. All flexibility is contained in two diametrically opposed appendages affixed to the central body. Furthermore, the appendages are considered to behave as rod-like members, such as booms or antennae.

Attitude perturbations from a desired reference position are counteracted by control jets supplying a pure torque, T_C, about the satellite centre. T_C can assume a positive or negative value, depending on the sense of the satellite's attitude angle. It is not necessary to consider any additional torques or forces for our purposes. Internal torques, due to fuel sloshing, friction, etc., are also considered beyond the scope of this analysis (Refs. 2 and 3 give an indication of the magnitudes of these additional torques.) Attitude information for the rigid main body is limited to one rotational degree of freedom, measured by θ. The lack of translational motion for the centre of mass immediately implies that symmetric modes of appendage flexure are being ignored. This results in no loss of generality for our purposes, since the symmetric modes do not affect θ.

A general control loop may be drawn for the system, as shown in Fig. 2. Attitude error, θ_E, is sensed by a controller which, in turn, applies a correcting torque to the satellite. The resulting motion of the body, which may be written as a superposition of rigid and flexible components, provides input to an attitude sensor feedback loop. In this study, it is assumed that the sensor processes the angle θ instantaneously, and with perfect accuracy. It is recognized that this latter assumption is quite idealistic and likely eliminates important instability possibilities; it is planned to remove this assumption in a subsequent study.

3. THE CONTROLLER

Though a simple controller model would be mathematically desirable, some sophistication is required in the simulation. It would be unrealistic, for example, to employ a basic relay-type controller. Such a system would provide a torque to counteract only the sense of θ_E. The jets, being non-throttling, would be constantly firing and expending fuel and thus an undesirable limit cycle would also be exhibited, as shown in Fig. 3(a), for a rigid system. Some improvement would be possible by providing a deadband region in the controller. No jet thrust would be applied while the attitude error was within certain bounds. However, fuel consumption would still be almost as high, and the limit cycle would also remain, see Fig. 3(b).

In order to achieve realistic performance in the simulation, it was decided to employ the slightly more complicated pseudo-rate (PSR) controller. A view of Fig. 3(c) illustrates typical PSR performance on a phase-plane plot. Velocities are quickly reduced, avoiding limit cycle instability.

3.1 Pseudo-Rate Control

The main feature of this nonlinear system is torque control through a form of pulse modulation. The spacecraft attitude control jets fire for brief intervals, reducing on-time, and therefore fuel requirements. Reference 4 provides the reader with more PSR information. Additional descriptions of ON-OFF controllers can be found in Ref.5. The width and frequency of the control pulses are determined by the attitude error angle, θ_E, and an artificially produced estimate of $\dot{\theta}_E$.

Figure 4 shows a schematic for the PSR controller. ϵ_1 is a function of the angle θ_E. The output, R (either -1, 0, or +1) acts as a switch for the torque jets. Some explanation of ϵ_3 is required. If the satellite were perfectly rigid, and had no initial angular velocity, then $\dot{\theta}$ would be calculable from the satellite's torque history.

$$\dot{\theta} \sim \int T_c \, dt$$

If we further assume the presence of ideal control jets, R will be related to T_c by a constant. ϵ_3, therefore, roughly approximates the time integral of R by virtue of the PSR feedback lag system. It is apparant that ϵ_3 can never be identically equal to velocity, due to the saturating effect of the lag network.

The feedback time constant, τ_f, often assumes two values, depending on whether the jets are on or off. This gives the control-system designer extra freedom for performance optimization. For our purposes, however, it will suffice to fix τ_f at one value only.

The limits of attitude error are defined by the bounds of the controller's deadband region. When θ_E exceeds this region, correcting torques may be applied. At either end of the deadband, a small area of hysteresis is found. These are particularly useful in reducing fuel consumption during limit cycle operation. This can occur, for example, under the influence of an external disturbance torque.

3.2 Controller Characteristic Frequency

It is possible to define a convenient "characteristic frequency" for the pseudo-rate control system. This derivation follows closely that shown in Ref. 4, and provides a useful reference base with which to reduce later data.

For small angular velocities about one axis, a linearized rigid equation of motion may be written:

$$I \ddot{\theta} = T_{eff} \tag{3.1}$$

where I and T_{eff} are the total inertia and effective control torque, respectively.

The effective torque will be a function of reaction jet torque, and the fraction of thruster on-time (duty cycle):

$$T_{eff} = T_c \frac{t_{on}}{t_{on} + t_{off}} = T_c r$$

Thus:

$$I \ddot{\theta} = T_c r \tag{3.2}$$

Consider again Fig. 4. Let us assume, for the moment, that ϵ_1 is a constant. This will be valid if the satellite dynamics respond slowly compared to thruster on-time. We may then write:

$$\epsilon_2 = K_f + (\epsilon_{2o} - K_f)\exp(-t/\tau_f) \tag{3.3}$$

where ϵ_{2o} is the initial value of ϵ_2. The switch turns on when $\epsilon_3 = 1$, and turns off when $\epsilon_3 = 1 - H$. Substituting (3.3) into $\epsilon_3 = \epsilon_1 - \epsilon_2$, we have:

$$1 - H = \epsilon_1 - K_f - (\epsilon_{2_o} - K_f)\exp(-t_{on}/\tau_f)$$

After rearranging:

$$t_{on} = \tau_f \, \ell n \left(\frac{K_f - \epsilon_{2_o}}{K_f + 1 - H - \epsilon_1} \right)$$

During steady state operation, $\epsilon_{2_o} = \epsilon_1 - 1$, at the time of pulse turn on.

Thus in the steady state:

$$t_{on} = \tau_f \, \ell n \left(\frac{K_f + 1 - \epsilon_1}{K_f + 1 - H - \epsilon_1} \right) \tag{3.4}$$

When the switch turns off,

$$\epsilon_3 = 1 - H = \epsilon_1 - \epsilon_2$$

The feedback circuit will decay according to the equation:

$$\epsilon_2 = \epsilon_{2_o} \exp(-t/\tau_f)$$

where $\epsilon_{2_o} = \epsilon_1 - (1 - H)$.

The switch will turn on again when:

$$\epsilon_3 = 1 = \epsilon_1 - \epsilon_{2_o} e^{-t_{off}/\tau_f}$$

After some rearranging:

$$t_{off} = \tau_f \, \ell n \left(\frac{\epsilon_1 - 1 + H}{\epsilon_1 - 1} \right) \tag{3.5}$$

If we now allow ϵ_1 to change slowly, we have

$$\epsilon_1(t + \Delta t) = \epsilon_1(t) + \Delta t \, \dot{\epsilon}_1(t) + \ldots$$

Substitute into (3.5)

$$t_{off} = \tau_f \, \ell n \left(1 + \frac{H - t_{off} \, \dot{\epsilon}_1}{\epsilon_1 + t_{off} \, \dot{\epsilon}_1 - 1} \right)$$

Since H and $\dot{\epsilon}_1$ are small, and provided that $\epsilon_1 > 1$, the logarithm may be expanded to give:

$$t_{off}(\epsilon_1 - 1 + t_{off} \, \dot{\epsilon}_1 + \tau_f \, \dot{\epsilon}_1) \approx \tau_f H$$

If we take $t_{off} \ll \tau_f$, then

$$t_{off} = \frac{\tau_f H}{\epsilon_1 - 1 + \tau_f \, \dot{\epsilon}_1} \tag{3.6}$$

From (3.4), the on-time may be similarly approximated:

$$t_{on} = \frac{\tau_f H}{K_f + 1 - H - \epsilon_1} \tag{3.7}$$

provided that $\epsilon_1 < K_f + (1 - H)$, that is, less than the saturation level.

The duty cycle was defined as:

$$r = \frac{t_{on}}{t_{on} + t_{off}}$$

In a well designed controller, $t_{on} \lll t_{off}$. Thus,

$$r \approx \frac{t_{on}}{t_{off}}$$

Substituting (3.6) and (3.7):

$$r = \frac{\epsilon_1 - 1 + \tau_f \dot{\epsilon}_1}{K_f + 1 - H - \epsilon_1}$$

Let us assume that the input is much greater than the deadband, and well below the saturation level. (This approximation would be invalid for limit cycle operation.)

$$1 \ll \epsilon_1 \ll K_f + (1 - H)$$

The H may be removed if the deadband is very small, i.e., $H \ll 1$. The following simplifications result:

(i) $$\epsilon_1 - 1 \approx \epsilon_1$$

(ii) $$K_f + 1 - \epsilon_1 \approx K_f$$

Substituting into the duty cycle equation, we find,

$$r = \frac{1}{K_f} (\epsilon_1 + \tau_f \dot{\epsilon}_1)$$

We may now back substitute into (3.2):

$$I \ddot{\theta} = \frac{T_c}{K_f} (\epsilon_1 + \tau_f \dot{\epsilon}_1) \tag{3.8}$$

ϵ_1 is related to θ through an amplifier of gain K_θ. Thus:

$$\epsilon_1 = - K_\theta \theta$$

Substitute into (3.8), and rearrange:

$$\ddot{\theta} + \frac{T_c K_\theta \tau_f}{I K_f} \dot{\theta} + \frac{T_c K_\theta}{I K_f} \theta = 0$$

The undamped natural frequency of the satellite system thus becomes:

$$\omega_c = \sqrt{\frac{T_c K_\theta}{I K_f}}$$

The characteristic frequency above allows us to define also a characteristic period of the form:

$$t^* = 2\pi \sqrt{\frac{I K_f}{T_c K_\theta}}$$

3.3 Test of ω_c and t*

The natural frequency and period, ω_c and t*, form basic measuring tools with which later data are reduced. It is, therefore, imperative to discover just how universal these characteristic values really are. A number of computer simulations were undertaken of the control system in Fig. 4. All parameters in the system were individually varied, and a plot was made of response vs. t/t* (i.e., multiples of the characteristic period). For t* to truly be a natural period, all plots should have similar period with respect to t/t*.

Sample plots are shown in Fig. 5, for a variation in the feedback time constant, τ_f. It is seen that the first quarter periods cluster about t/t* = 0.25, as desired, although subsequent period fractions tend to deviate from their predicted values. Plots investigating other control loop parameters showed very similar patterns. The consistency of these results, though only for the first quarter period, demonstrates that our definition of t* (and therefore ω_c) does indeed produce a characteristic parameter.

4. THE DYNAMICS BLOCK

The vehicle dynamics portion of the control loop describes the structural response of the satellite model. The transfer functions therein allow for rigid and flexible contributions to the total motion. (Ref. 9 provides an informative overview.) The flexible motions are initially confined to linear and nondissipative elastic effects. Linearity is mathematically preserved by restricting motions to small scale deflections. This restriction is not considered serious, since modern satellite control systems are designed for small attitude excursions. The assumption of linearity in the structural response considerably simplifies the mathematical formulation of the model since the problem is then amenable to a convenient modal analysis.

4.1 Modes

The equations of motion for our satellite model may be derived either through classical continuum mechanics theory (e.g., Ref. 7), or more modern methods (e.g., finite elements). In the former case, partial differential equations may initially be written in space and time variables. Separation of variables is then employed to isolate the (sinusoidal) time-dependent portion from the space-dependent (modal) portion. Results resolve into an eigenvalue problem, with the eigenvalues and eigensolutions indicating individual modal frequencies and shapes. The solution is typically of the form:

$$Y(x,t) = \sum_{n=1}^{\infty} \delta_n(x) q_n(t)$$

where $\delta_n(x)$ is the n^{th} normalized mode of the complete system, and

$q_n(t)$ is the time dependent generalized displacement coordinate associated with the n^{th} mode.

For a general discussion of these matters, the reader is referred to Ref. 6.

It is apparent that the deflection $Y(x,t)$ can be related to the attitude angle θ of the rigid core. It can also be seen that θ will be composed of contributions due to the various modes. We may write:

$$\theta = \Theta + \sum_{n=1}^{\infty} \theta_n q_n(t)$$

where Θ is the main body angle due to rigid motions;

$\theta_n q_n$ is the attitude angle contribution from the n^{th} mode.

The modal deflections are typically of the form shown in Fig. 6. In theory, there are an infinite number of shapes, corresponding to the infinite number of eigenfunctions. Half of these will be symmetric motions, involving no angular displacement of the central body. These, as mentioned previously, are of no direct interest in the present context.

Of the remaining infinite number of antisymmetric modes, only the first few would be of any importance. It is unlikely that the higher frequency modes would be excited by disturbances that a real spacecraft would encounter. Furthermore, higher order motions would tend to be transparent to the control circuit, due to the filtering effect of the attitude sensor.

4.2 Flexibility Parameters (k and ω)

Each characteristic motion will contribute its own dynamic effects to the control loop. For the purposes of a mathematical simulation, it is advantageous to describe these effects in terms of two basic parameters. The first, ω, is the previously mentioned modal frequency. The second may be termed the modal gain, k. Loosely speaking, the gains will indicate the fraction of attitude acceleration attributable to individual modes.

Each flexible mode, as represented by ω and k, contributes to the transfer function acting upon a satellite's ideal rigid motion. The larger the value of k for any individual mode, the larger will be the influence of that mode. Reference 7 develops a number of formulae to estimate values for ω and k. However, before introducing these results, some further background is necessary.

4.3 Constrained and Unconstrained Parameters

Spacecraft designers have the option of defining satellite modes from two vantage points (Ref. 10). For satellites with a rigid main body and flexible appendages, it is possible to consider motions of the elastic members separately. This is equivalent to assuming a fixed central body. Actual main body motion may subsequently be modelled as driving forces to the appendages. Modes of this form are termed "constrained", and give rise to constrained frequencies and gains, Ω and K. Conversely, mode shapes of the complete satellite may be considered, with the main body free to rotate. These modes result in "unconstrained" frequencies and gains, ω and k.

The relationship between the two systems can be further appreciated through Figs. 7 and 8, where block diagrams are shown of constrained and unconstrained vehicle dynamics. The former involves a feedback mechanism to alter the rigid response, while the latter has a feed forward summation of modal contributions. Both formulations provide similar solutions provided that the number of modes considered is made sufficiently large.

According to Ref. 7, constrained frequencies for 'rod-like' flexible members follow the approximation:

$$\Omega_p \sim p^2 \qquad (p = 1, 2, 3\ldots) \tag{4.1}$$

where p represents the mode number. It is apparent that an equality can be made if any mode's natural frequency is known.

Once the Ω_p are found, the constrained gains for the rod-like appendages are approximated by:

$$K_p = 2.084 \frac{\beta}{\Omega_p^2} \tag{4.2}$$

where $\beta = I_f/I$ is the ratio of flexible inertia to the satellite's total inertia. The parameter β is a measure of the degree of flexibility in the vehicle. It is apparent that $0 \leq \beta \leq 1$.

To relate the constrained parameters to their unconstrained counterparts, we may make use of the following identities:

$$\sum_{p=1}^{\infty} \frac{K_p}{\omega_q^2 - \Omega_p^2} = \frac{1}{\omega_q^2} \tag{4.3}$$

$$\sum_{p=1}^{\infty} \frac{k_p}{\omega_p^2 - \Omega_q^2} = \frac{1}{\Omega_q^2} \qquad (4.4)$$

Vehicle dynamics computed using constrained parameters are found to have lesser accuracy near resonance than those calculated using an equal number of unconstrained modes. However, experience has shown that accuracies near resonance will be comparable if the number of constrained modes is made sufficiently larger than the number required in the unconstrained format.

5. THE FINAL COMPUTER MODEL

The full simulation block diagram, complete with controller and structural dynamics sections, is shown in Fig. 9. An unconstrained format was adopted for the body dynamics block, with modal parameters derived from a constrained system. This allowed greater accuracy than would have been possible with the constrained method, given a similar number of modes.

Only one flexible unconstrained mode was included with the rigid mode, in the interests of computational economy. It was not felt that this simplification would alter the basic character of the results.

5.1 Values of Controller Parameters

The choice of values for PSR parameters requires a detailed analysis by the satellite designer. The system must be optimized for performance, fuel economy, cost, etc.

In order to present a realistic system, it was deemed best to employ values designed for a practical spacecraft. In this regard, we were fortunate to have available an early design study (Ref. 4) of the back-up pitch controller for Canada's CTS satellite. The following parameters, originating in that report, were used in our model.

Parameter	Value
K_θ	163
K_f	13.3
H	0.0188
τ_f	8.8 sec.
K_{jet}	0.12 ft-lb
I	68 slug-ft^2

The system was designed for a deadband angle (DB) of 0.35 degrees.

In the simulation, a time integral was taken of the PSR relay output. Termed t_{on}, the value provided a measure of thruster on-time, and therefore an indication of fuel consumption.

5.2 Values of Flexibility Parameters

The modal frequency and gain for the unconstrained flexibility block were derived from an equivalent system of three constrained modes. A value of β and Ω_1 would be set for the first constrained mode. Equations (4.1) and (4.2) would then be employed to estimate the values of Ω and K for the first three constrained modes. These, in conjunction with the transform equations (4.3) and (4.4) then provided ω_1 and k_1 for the first unconstrained flexible mode. Thus, the two parameters β and Ω_1 could be thought of as defining a 'condition of flexibility' for the unconstrained dynamics block.

In this study, interest centres on appendage frequencies close to the satellite's control loop natural frequency. A parameter was defined to measure this feature. Expressed in terms of constrained or unconstrained frequencies it becomes, respectively,

$$\Phi = \frac{\Omega_1}{\omega_c}$$

or

$$\phi = \frac{\omega_1}{\omega_c}$$

Values of Ω_1 were restricted so that Φ would not exceed the range 0.1 to 10. Figure 10 shows the relationship of ϕ to Φ over the entire range of β. It is seen that ϕ approaches Φ as the value of β diminishes.

The presence of a damping parameter, ζ, in the flexibility block, requires some explanation. It is a standard, though mathematically non-rigorous, practice to include this energy dissipative term in dynamic simulations. This parameter has a small value, in practice. For our model, a value of 0.001 was chosen.

5.3 Nondimensionalization of Variables

Simulation variables which would be of later interest were made dimensionless, and denoted by the symbol ($\hat{}$). The following chart lists the nondimensionalizing factors:

Variables		Nondimensional Factor
time:	t, t_{on}	$(1/t^*)$
angles:	θ, $\theta_1 q_1$	$(1/DB)$
angle rate:	$\dot{\theta}$, $\theta_1 \dot{q}_1$	(t^*/DB)

DB and t^* refer to the deadband angle and characteristic time, respectively.

5.4 Initial Conditions

A number of initial conditions must be set for the integrating blocks. Conditions were made compatible with a step change from a motionless attitude. That is, q, $\dot{q}$, $\dot{\theta}_o$, were zero, while θ_o was given an arbitrary rotation of 10 DB.

6. COMPUTATION PROCEDURE

An IBM-packaged computer language named CSMP (Continuous System Modelling Program) was available to numerically solve the control loop equations. CSMP has the great advantage of being a digital dynamic simulation program, while offering many advantages of analog computation. In use, the programmer is simply required to list system transfer functions, and set the various numerical constants and initial conditions.

The CSMP user must pay the price, however, for the programming ease. Since the program is supplied as a prepackaged language, the programmer must arrange his problem to suit the program, and not vice-versa. Input and output formats are limited, as are the variables available as output. Another disadvantage is the large amount of compiling time required to process a CSMP simulation.

The particular program written to solve the system of Fig. 9 is found in Appendix A. Most of the statements are self-explanatory. Two subprograms are added; one simulates the PSR relay with deadband and hysteresis, while the other provides punched cards of required output variables.

6.1 Integration Method

A CSMP-supplied fifth-order Milne method was selected for integration. Step size was allowed to vary, being decreased until prescribed error criteria were met.

Predictor and corrector calculations were applied by CSMP, using the following formulae:

Predictor:

$$Y^P(t + \Delta t) = Y(t - \Delta t) + (\Delta t/3)[8X(t) - 5X(t - \Delta t) + 4X(t - 2\Delta t) - X(t - 3\Delta t)] \quad (6.1)$$

Corrector:

$$Y^C(t + \Delta t) = \frac{1}{8}[Y(t) + 7Y(t - \Delta t)] + \frac{\Delta t}{192}[65X(t + \Delta t) + 243X(t) + 51X(t - \Delta t) + X(t - 2\Delta t)] \quad (6.2)$$

The integration interval was then adjusted, such that one of the following equations would be satisfied:

$$\frac{0.04\,|Y^C - Y^P|}{|Y^C|} \leq A; \qquad |Y^C| > 1 \qquad (6.3)$$

or

$$0.04\,|Y^C - Y^P| \leq A; \qquad |Y^C| \leq 1 \qquad (6.4)$$

where A is the allowable error.

Once these criteria were satisfied, the integration estimate became:

$$Y(t + \Delta t) = 0.03884\ Y^P(t + \Delta t)$$

6.2 Operating Procedure

The CSMP program was run to provide output from $t = 0.0$ to $t = 20.0$. (This corresponds to $t \approx 855$ seconds of real time.) With each run, new values were set for the flexibility parameters ω_1 and k_1 corresponding to a predetermined Φ and β. β was varied from 0.1 to 1.0 in steps of 0.1. Φ took on five values in the range 0.1 to 10.0. This resulted in a total of 50 simulations with flexibility, in addition to one rigid reference case.

A number of simulations were undertaken to determine a reasonable error criterion. It was found that an error of 5×10^{-6} was required at large β and Φ to find output approaching a limit. At lower values of β and Φ, the error could be relaxed to 1×10^{-4}, allowing better computational economy. Computer CPU times on the University of Toronto's IBM 370 system were generally in the range of 0.25 to 0.70 minutes per simulation.

7. DATA PRESENTATION AND ANALYSIS

Punched card output from the CSMP program provided values of $\hat{t}$, $\hat{\theta}$, $\mathring{\hat{\theta}}$, $\hat{\theta}_1$, $\mathring{\hat{\theta}}_1$, and $\hat{t}_{on}$ at regular small intervals of time. These provided the data base from which simulations were analyzed. From here on, we write simply θ_1 for $\theta_1 q_1$.

7.1 Simulation Plots

To allow a qualitative overview of performance trends, a number of computer plots were drawn of each simulation run. The attitude angle and rate, $\hat{\theta}$ and $\mathring{\hat{\theta}}$ were plotted versus $\hat{t}$, as was the measure of fuel consumption, $\hat{t}_{on}$. ($\hat{t}_{on}$ was divided by the value of $\hat{t}_{on}$ for the rigid spacecraft to give a "fuel factor".) A step-by-step calculation of satellite mechanical energy was also plotted against $\hat{t}$. (The formula used is presented in Appendix B.) This display is particularly valuable, since it provides some insight into stability. The more rapidly the vehicle loses its mechanical energy, the more quickly it approaches its ideal ultimate state of zero $\mathring{\theta}$ and zero θ. Clearly if the energy were to steadily increase, the satellite configuration could be labelled unstable. This would indicate that energy from control jet pulses was being added to attitude oscillations, instead of being subtracted, as required.

Figures 11 through 31 show some of the simulation plots. The first of the series, Fig. 11, presents the performance of the fully rigid spacecraft ($\beta = 0$). Following are graphs at $\beta = 0.1$, 0.4, 0.7, and 1.0 for the full range of Φ. A number of trends are evident.

$\hat{\theta}$ vs $\hat{t}$

All simulations show a rapid initial reduction of θ to values hovering about the deadband. There are pattern changes, though, that relate to ranges of Φ. At low Φ, the attitude angle tends to ride the edge of the deadband. It appears that the control jets have the power to hold the main body in place, but must constantly fight the slowly but surely moving appendages. When Φ is greater than 1.0 (above controller resonance), the response tends to follow the rigid simulation pattern. The flexible vibration of the booms seems to add only a high-frequency ripple to a steady motion, as shown for the case $\beta = 0.1$, $\Phi = 3.16$. Unlike the lower frequency examples, the response of the appendages does not dominate the pattern.

$\dot{\hat{\theta}}$ vs $\hat{t}$

The oscillatory frequency is readily apparent in these plots. Like the displacement vs time series, the response pattern is more a function of Φ than it is of β. At low values of Φ, the pattern follows the form of alternating spikes about a relatively low velocity. The steady low velocity corresponds to the intervals where θ hugs the deadband edge. The large spikes show the effect of the appendages intermittently swinging the core to the opposite side of the deadband. Velocities will be high until the thruster fires repeatedly, again bringing the attitude angle to the deadband edge. For the larger Φ's, there is a ripple of varying magnitude about steady coasting velocities.

$\hat{t}_{on}$ vs $\hat{t}$

Fuel usage at larger values of Φ follows closely the figure for the rigid satellite. The thruster uses little power after $t = 2.0$. This contrasts sharply to the requirement of satellites with $\Phi = 0.1$. After the initial spurt of fuel, the usage figure slowly, but steadily, increases. The total flow at $\hat{t} = 20$, however, remains somewhat lower. The largest figures for fuel usage are found when the satellite's natural frequency is approached, and especially for large β. Similar to the low frequency case, a large portion is spent after the initial jump.

Energy vs $\hat{t}$

There seem to be three patterns for the energy plots. At low Φ, there is a tendency to drop rapidly to a high and steady value. This indicates that the attitude jets have little effect on the vibrations of the low frequency appendages, once those appendages have been set in motion.

At the slightly larger frequency of $\Phi = 0.316$, the energy follows a slow steady decrease, showing some controller effectiveness in reducing vibration.

For $\Phi = 10.0$ and for $\Phi = 3.16$ at high β, there is a rapid decrease to a low energy value. Being comparable to the rigid case, it provides an extra indication that little flexible vibration occurs at large Φ.

7.2 Performance Quality Numbers

The simulation data was subjected to a more quantitative analysis through a program called "SIGVALS". This program, found in Appendix A, isolated or calculated values from the simulations which were considered significant in terms of showing satellite performance. The items of interest were:

(i) Total Fuel Expended

The total thruster-on time for each flexible simulation was divided by the corresponding $\hat{t}_{on}$ for the rigid satellite. This provided a fuel factor corresponding to the fuel used in a particular run, divided by the fuel usage for the reference rigid run.

(ii) Time in Deadband

The primary function of the control system is to maintain the attitude angle, θ, within the deadband region. A measure of the system's success in meeting this requirement is shown by the percent of time that it actually satisfies $|\hat{\theta}| < 1.0$.

(iii) Initial Overshooting

When the control loop is first excited, there is a tendency for state variables to overshoot. A satellite with less overshoot is better capable of coping with attitude perturbations. Program SIGVALS, therefore, was designed to find the maximum overshoot of the attitude angle and rate ($\hat{\theta}$ and $\hat{\dot{\theta}}$), along with the component of angle and rate due to flexibility ($\hat{\theta}_1$ and $\hat{\dot{\theta}}_1$).

(iv) Secondary Maximums of Variables

In the time span of $\hat{t} = 2.0$ to the final $\hat{t} = 20.0$, it can be assumed that initial overshooting has tapered away. The maximum magnitudes of the state variables now provide some indication of deviation over an extended period.

(v) Energy

Ultimately, the energy represented by the state variables should become zero. How closely a given simulation approaches this goal indicates system stability. By calculating the energy at $\hat{t} = 20.0$, a powerful indicator of performance quality was measured.

7.3 Plots of Performance Quality Regions

The "significant numbers" found above for each simulation were assessed. Grades were assigned, ranging in value from "A" to "E", with an A identifying the best level. Generally, an "A" signified performance equal to, or better than, the performance of the rigid reference case. Each performance criteria of Section 7.2 received a quality grading for all flexible simulations. This allowed quality region plots to be drawn, as shown in Fig. 32 to 38. (The computer program which calculated the quality grading, and drew the plots is found in Appendix A.) Each criterion has a display of Φ vs β. Quality gradings are entered in the position corresponding to each simulation's flexibility parameters.

Figure 32 shows plots for criterion 1 using both the constrained and unconstrained format (i.e., Φ vs β and ϕ vs β). Subsequently, only the unconstrained type is displayed. The latter can easily be converted, using the transformation of Fig. 10.

8. RESULTS FROM PERFORMANCE ANALYSIS

Figures 32 through 38 show many interesting performance trends for the flexible satellite model. Each criterion of quality will be reviewed individually.

Criterion 1. Fuel Expended

There is a definite increase in fuel consumption as the appendage modal frequency approaches the satellite's natural frequency (i.e., $\phi \approx 1.0$). In addition, extra fuel is required at large β. The excellent economy shown at low ϕ may be misleading, however, due to the finite interval of our simulations. The fuel usage plots show little sign of easing consumption at $\hat{t} = 20.0$, indicating that larger long term figures can be expected.

Criterion 2. Time in Deadband

A definite trend is shown of decreasing deadband time as ϕ decreases, and as β increases. Only those frequencies above ω_c show good results.

Criterion 3. $\hat{\theta}$ Overshoot

The attitude angle is shown to be less likely to overshoot at large β and small ϕ. This β trend is due, no doubt, to the decreased main body inertia which the attitude jets must control. The lower frequency of vibration allows plenty of time for the jets to assert authority.

Criterion 4. $\hat{\dot{\theta}}$ Overshoot

The area of highest velocity overshoot is found at low ϕ and large β. Most of the performance degradation is caused by the worsening contribution of $\dot{\theta}_1$ (see Criterion 6 below).

Criterion 5. $\hat{\theta}_1$ Overshoot

The trend in this criterion is exactly opposite to that observed in Criterion 3. The implication is apparent. The proportion of appendage inertia is largest when the rigid main body inertia is least, making the high β, low ϕ, zone most subject to overshoot.

Criterion 6. $\hat{\dot{\theta}}_1$ Overshoot

The region of high $\hat{\dot{\theta}}_1$ overshoot is also the region of largest $\hat{\theta}_1$. The larger flexible displacements at given frequencies result in correspondingly larger modal velocities.

Criterion 7. Secondary $\hat{\theta}$

The long-term attitude angle perturbations become considerably degraded around the resonance frequency. Good performance is found only at the high and low modal frequencies.

Criterion 8. Secondary $\hat{\dot{\theta}}$

The trends of the velocity excursions follow closely the pattern established above for the angular displacements.

Criterion 9. Secondary $\hat{\theta}_1$

The simulation plots of Figs. 11 to 31 showed how the appendage motion became more violent at low ϕ and high β. This is distinctly underlined by the larger long term $\hat{\theta}_1$ in this regime, as shown in the performance quality plot.

Criterion 10. Secondary $\hat{\dot{\theta}}_1$

Areas of highest appendage velocity, $\hat{\dot{\theta}}_1$, coincide with the regions of maximum $\hat{\theta}_1$. This is compatible with the results of Criterion 9.

Criterion 11. Energy at $\hat{t} = 20$

The quality pattern found for the energy criterion is not as clear as some others. However, one result is readily apparent. At ϕ above the resonant frequency, energy drops very well, with somewhat less improvement at smaller β.

The low frequency, high flexibility region (low ϕ, high β) retains a large amount of residual energy.

8.1 Concluding Remarks

The plots of the preceding section show definite variations in satellite performance as a function of appendage flexibility.

The ability of the pseudo-rate controller to operate well is very much a function of the natural frequency of vibration of the appendages. At higher frequencies, the elastic modes are not as likely to become excited by control inputs. At lower ranges, however, elastic oscillations can become a dominant motion, particularly when large boom inertias are present. In addition, these modes tend to persist much longer, as shown by the energy plots.

It is of marked interest that energy levels for all simulations show a decreasing trend with time. This indicates that no unstable behaviour has been found for any flexible condition of our spacecraft model.

REFERENCES

1. Likins, P. W.; Bouvier, H. K. — "Attitude Control of Nonrigid Spacecraft", Astronautics and Aeronautics, May 1971.

2. Greensite, A. L. — "Analysis and Design of Space Vehicle Flight Control Systems", Vol. XII, NASA CR-831.

3. Deutsch, R. — "Orbital Dynamics of Space Vehicles", Prentice-Hall, Inc., New Jersey, 1963.

4. Staley, D. A. — SPAR Interoffice Memo, Oct. 12, 1971.

5. Greensite, A. L. — "Analysis and Design of Space Vehicle Flight Control Systems", Vol. IV, NASA CR-823.

6. Likins, P. W. — "Dynamics and Control of Flexible Space Vehicles", JPL Tech. Report No. 32-1329, Rev. 1, Jan. 1970.

7. Hughes, P. C.; Garg, S. C. — "Dynamics of Large Flexible Solar Arrays and Application to Spacecraft Attitude Control System Design", UTIAS Report 179, Feb. 1973.

8. NASA — "Effects of Structural Flexibility on Spacecraft Control Systems", NASA SP-8016.

9. Gevarter, W. B. — "Basic Relations for Control of Flexible Vehicles", AIAA Journal, April 1970.

10. Hughes, P. C. — "Dynamics of Flexible Space Vehicles with Active Attitude Control", Celestial Mechanics Journal, Vol. 9, pp. 21-39, 1974.

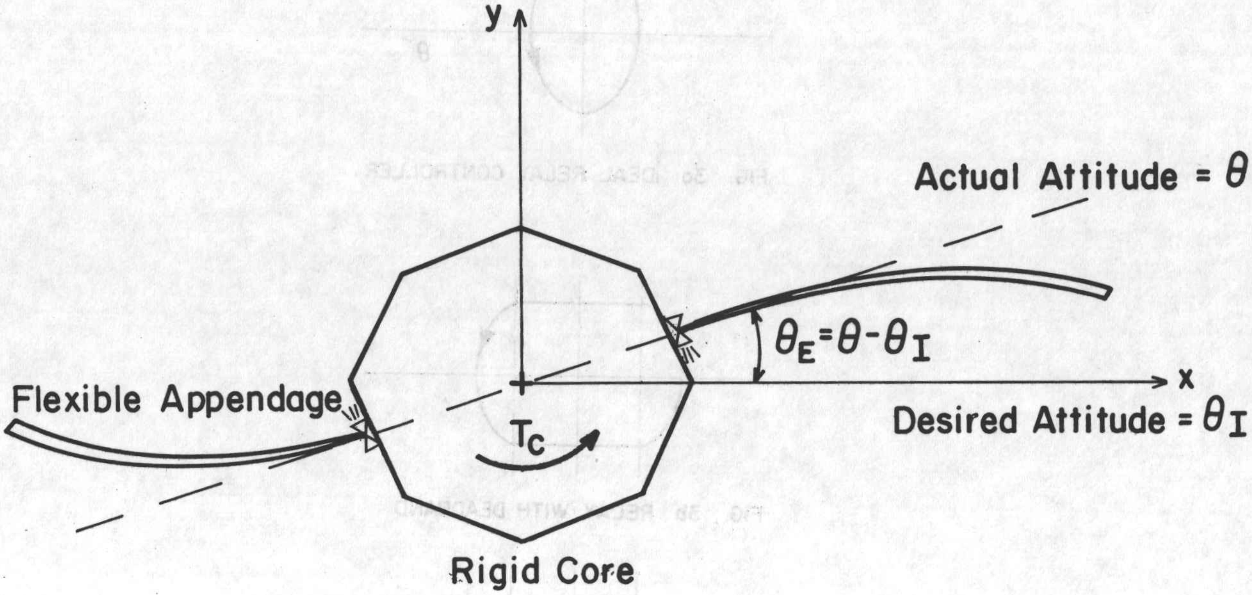

FIG. I SATELLITE GEOMETRY

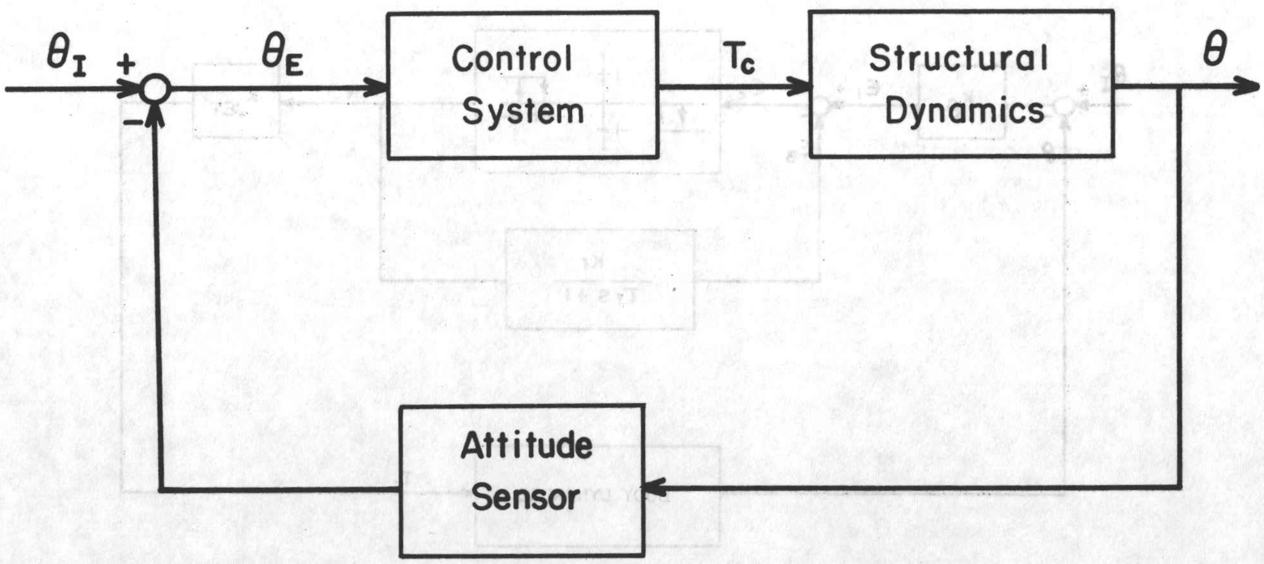

FIG. 2 GENERAL CONTROL LOOP

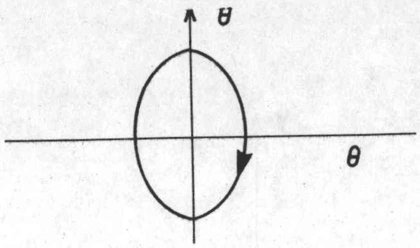

FIG. 3a IDEAL RELAY CONTROLLER

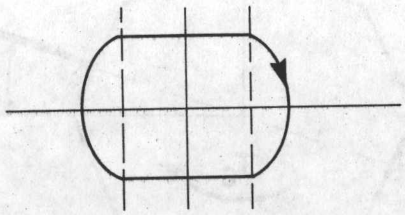

FIG. 3b RELAY WITH DEADBAND

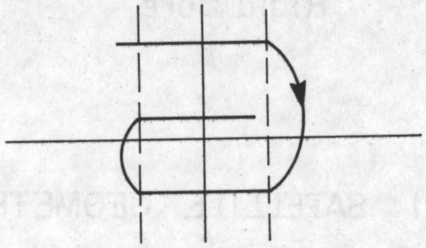

FIG. 3c PSR CONTROL

FIG. 3 PHASE PLANE PORTRAITS OF SEVERAL CONTROLLERS
(RIGID SATELLITE)

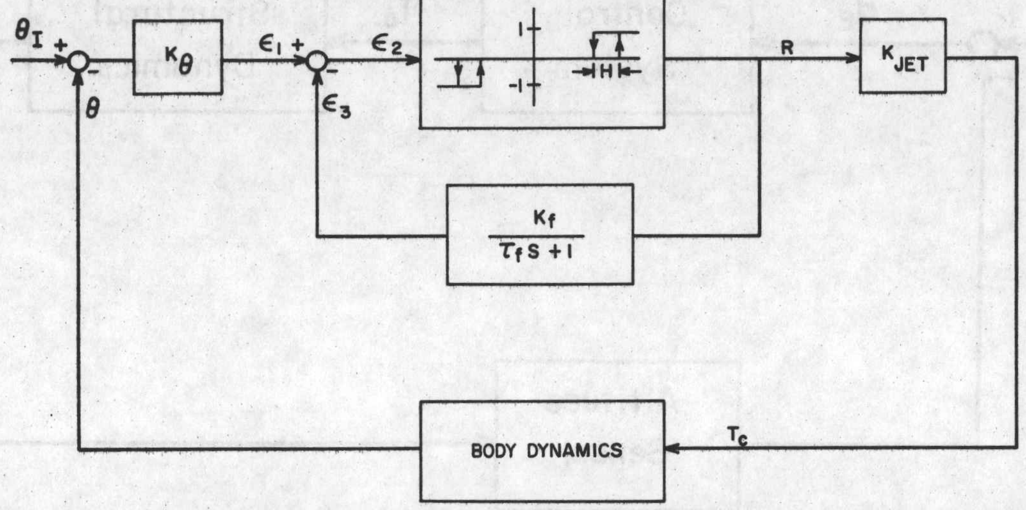

FIG. 4 PSR CONTROLLER

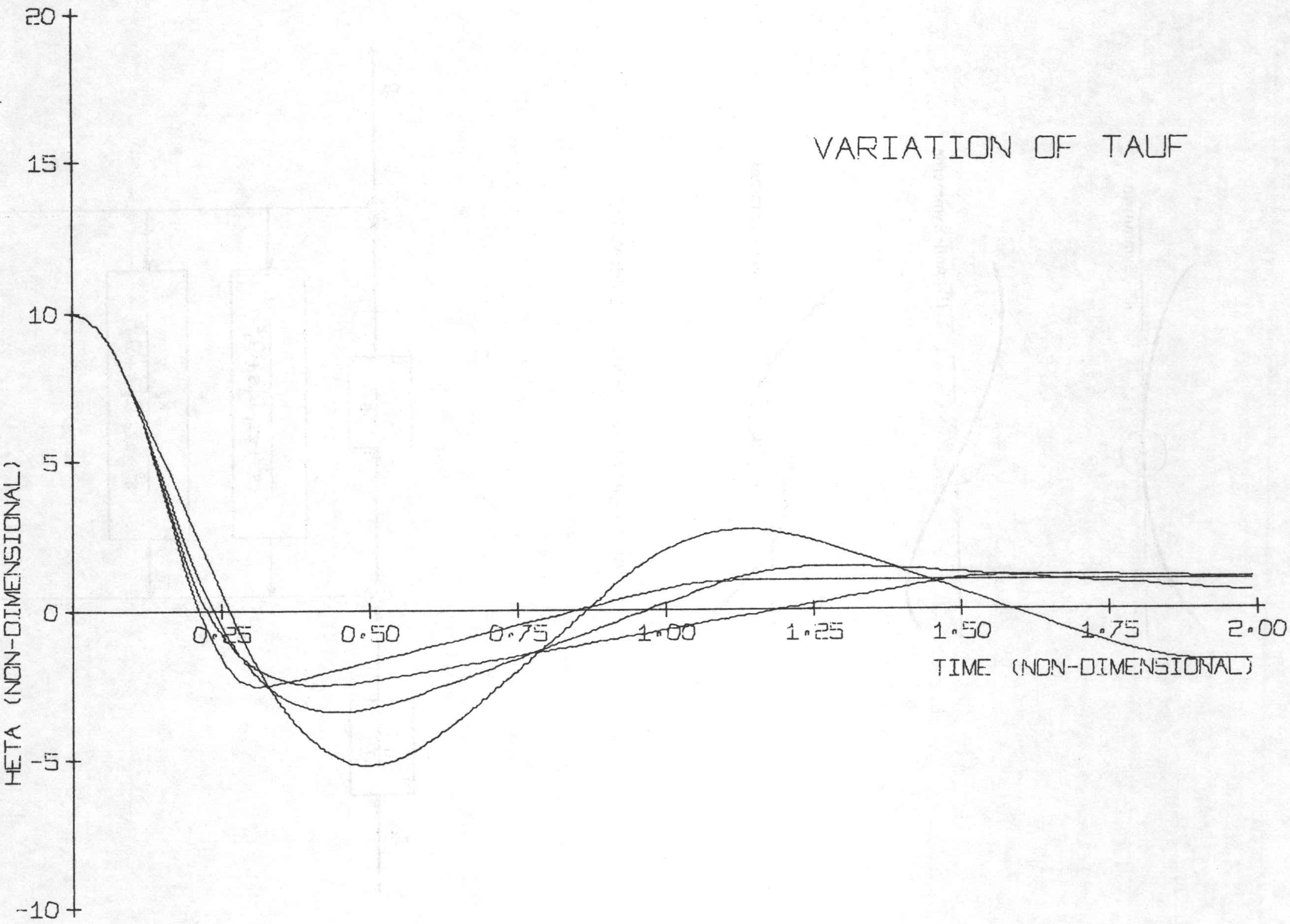

FIG. 5 RIGID SYSTEM RESPONSE

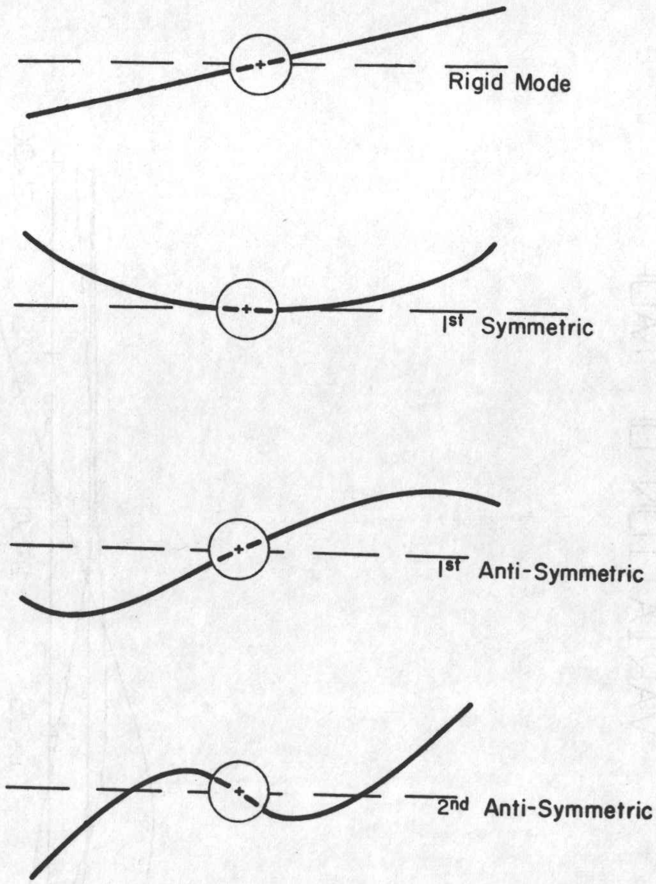

FIG. 6 NATURAL FLEXIBLE MODES (SCHEMATIC)

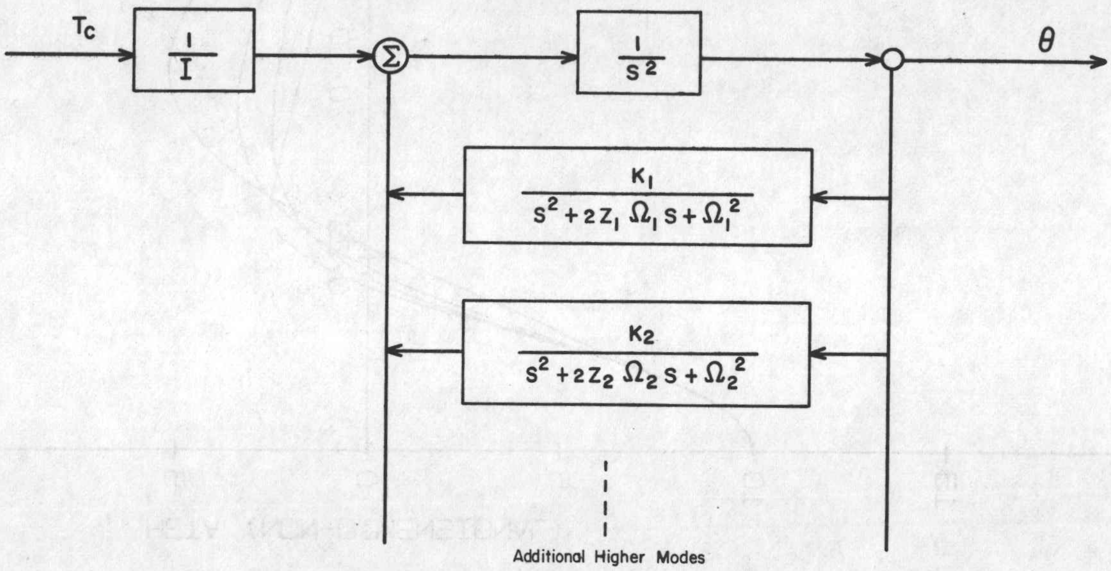

FIG. 7 BLOCK DIAGRAM OF CONSTRAINED DYNAMICS

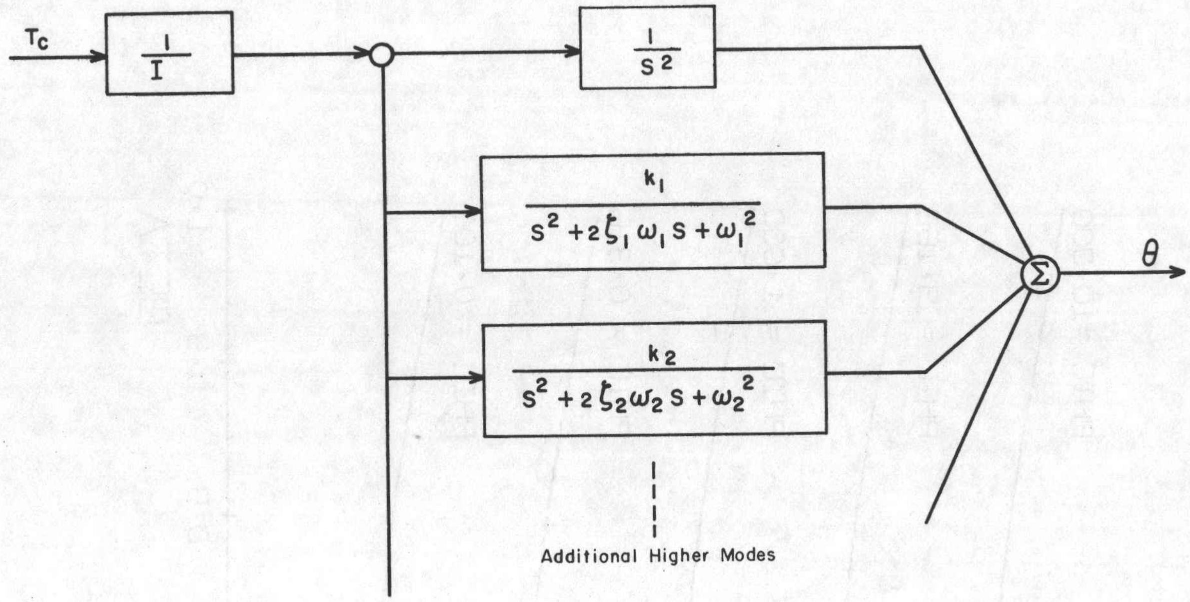

FIG. 8 BLOCK DIAGRAM OF UNCONSTRAINED DYNAMICS

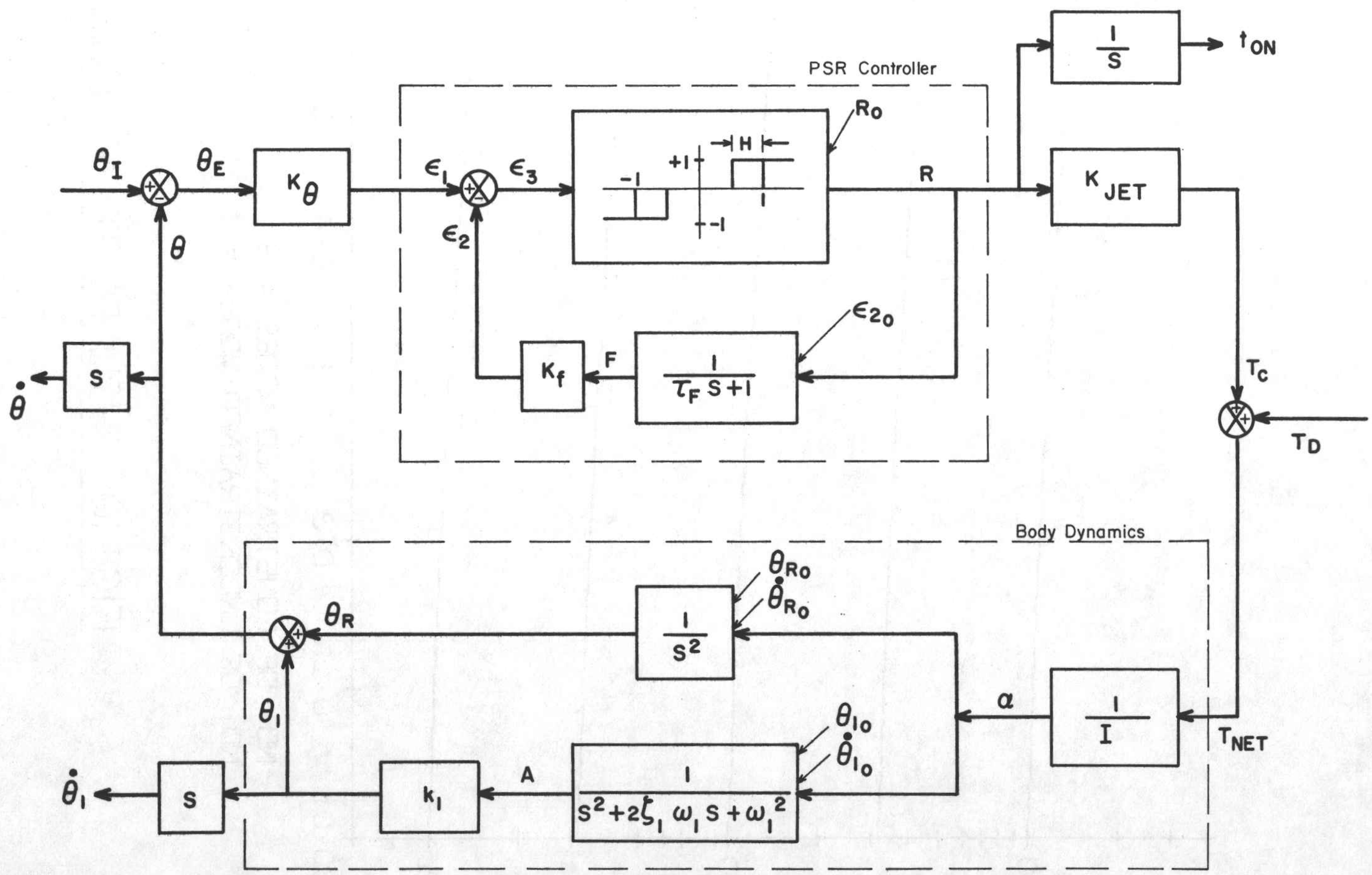

FIG. 9 SIMULATION BLOCK DIAGRAM

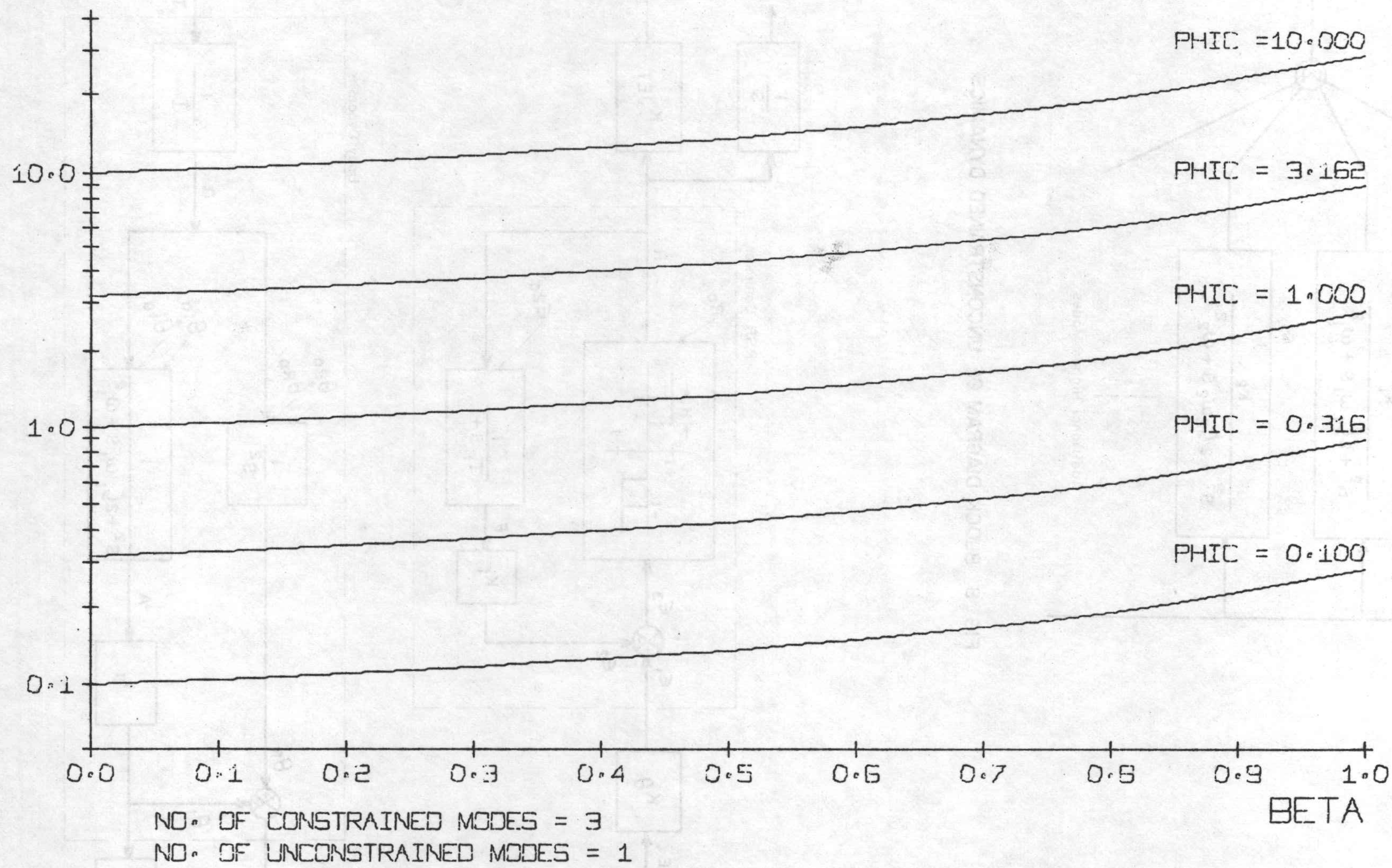

FIG. 10 PHIU PLOT AT CONSTANT PHIC

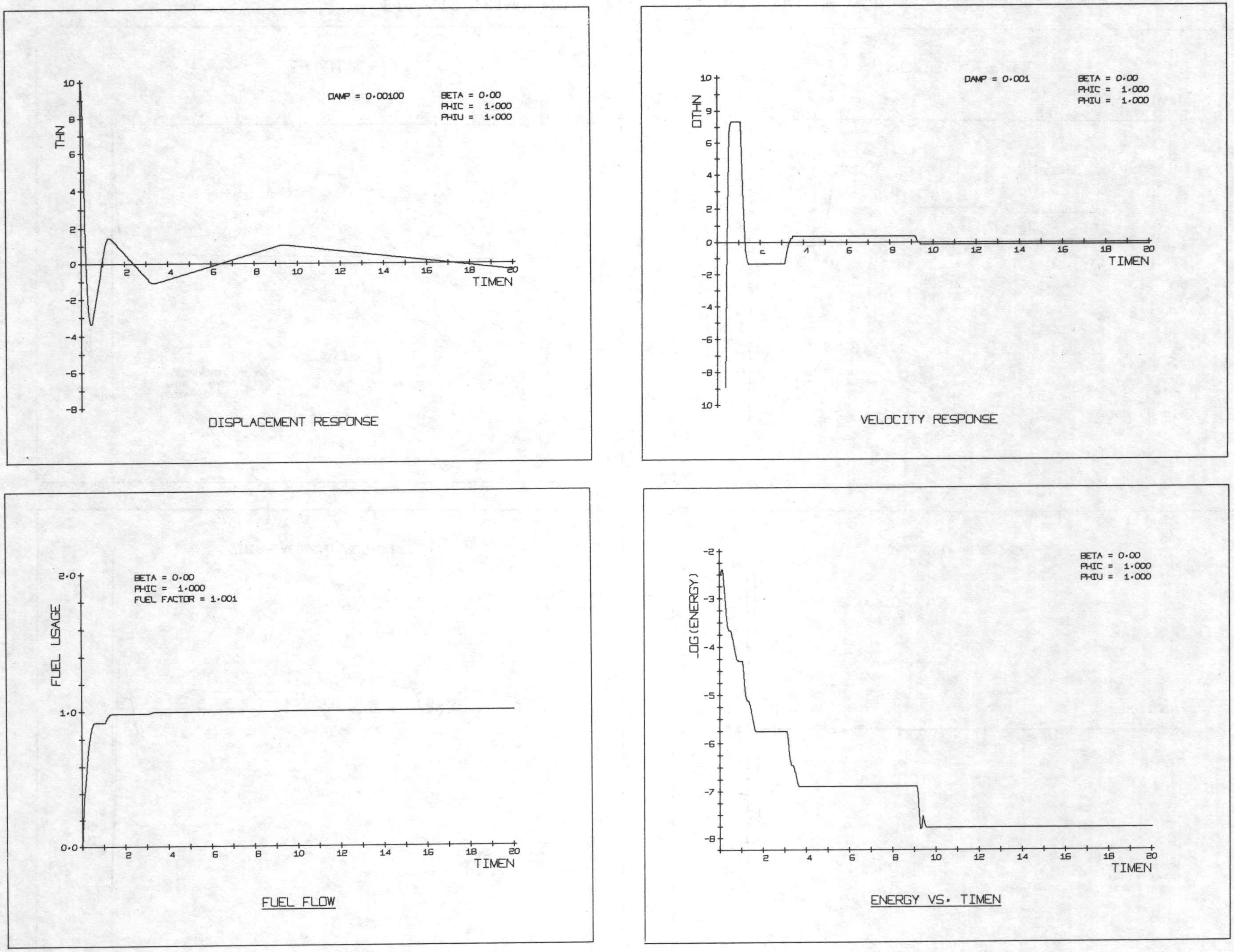

FIG. 11 SIMULATION AT BETA = 0.0, PHIC = 1.0

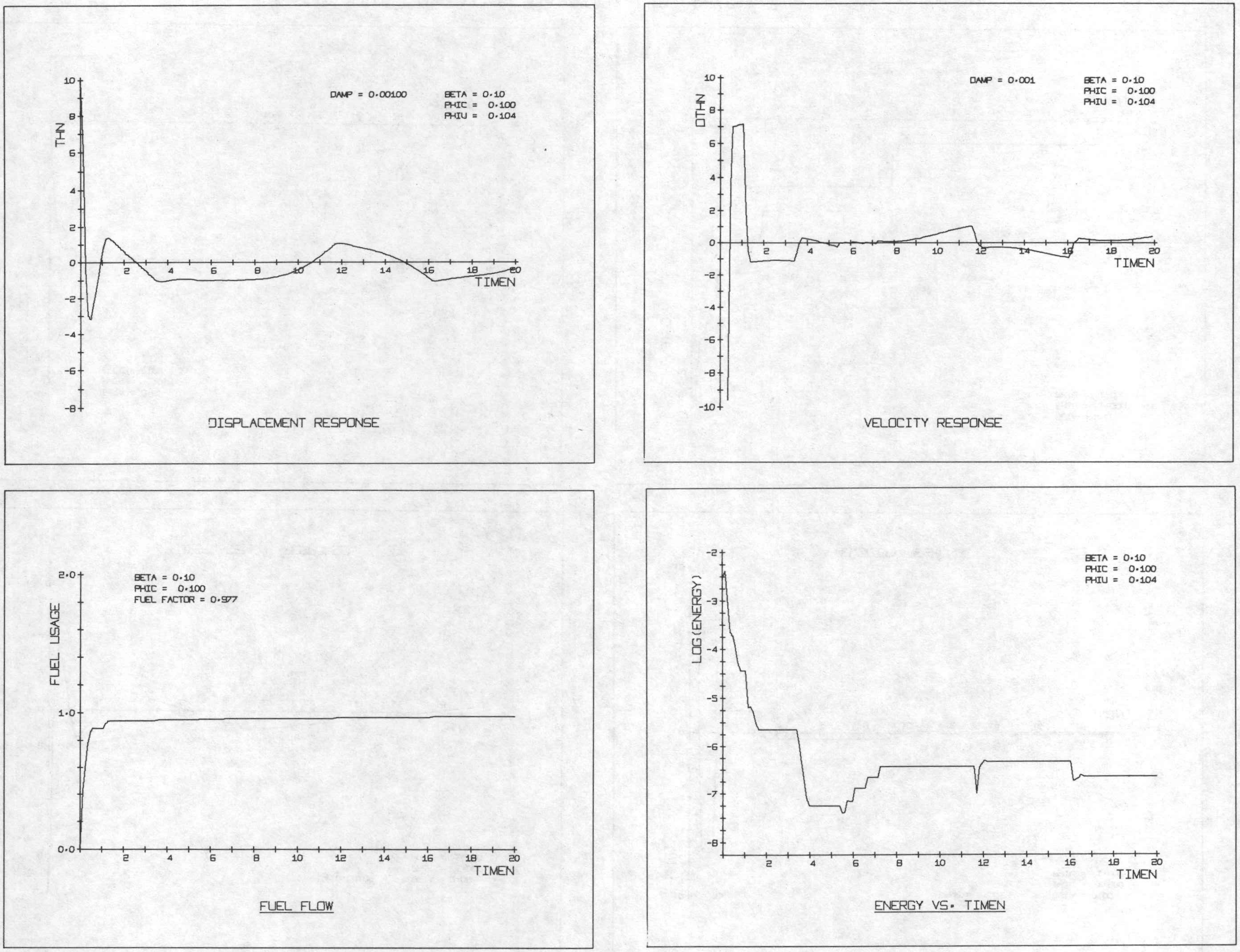

FIG. 12 SIMULATION AT BETA = 0.1, PHIC = 0.1

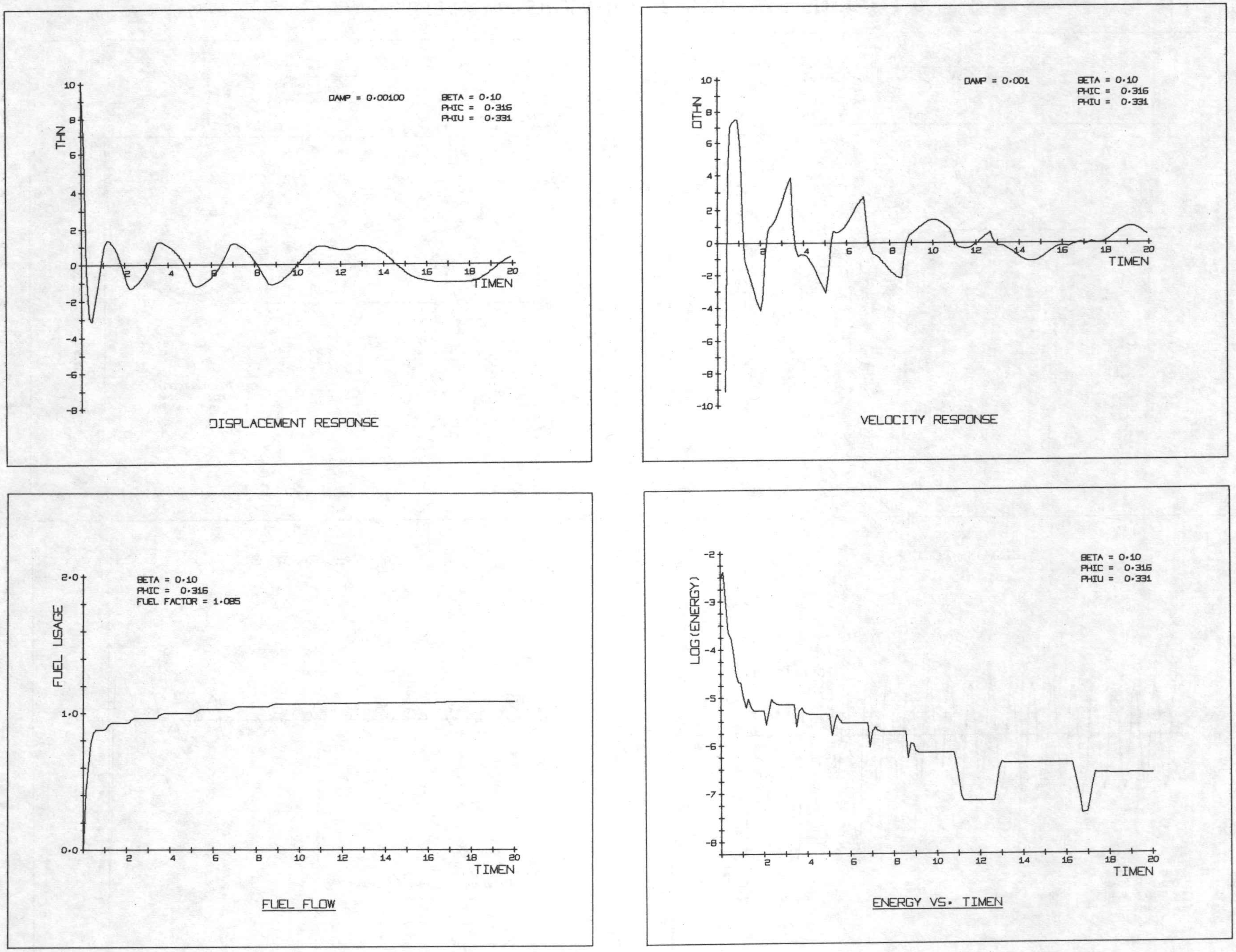

FIG. 13 SIMULATION AT BETA = 0.1, PHIC = 0.316

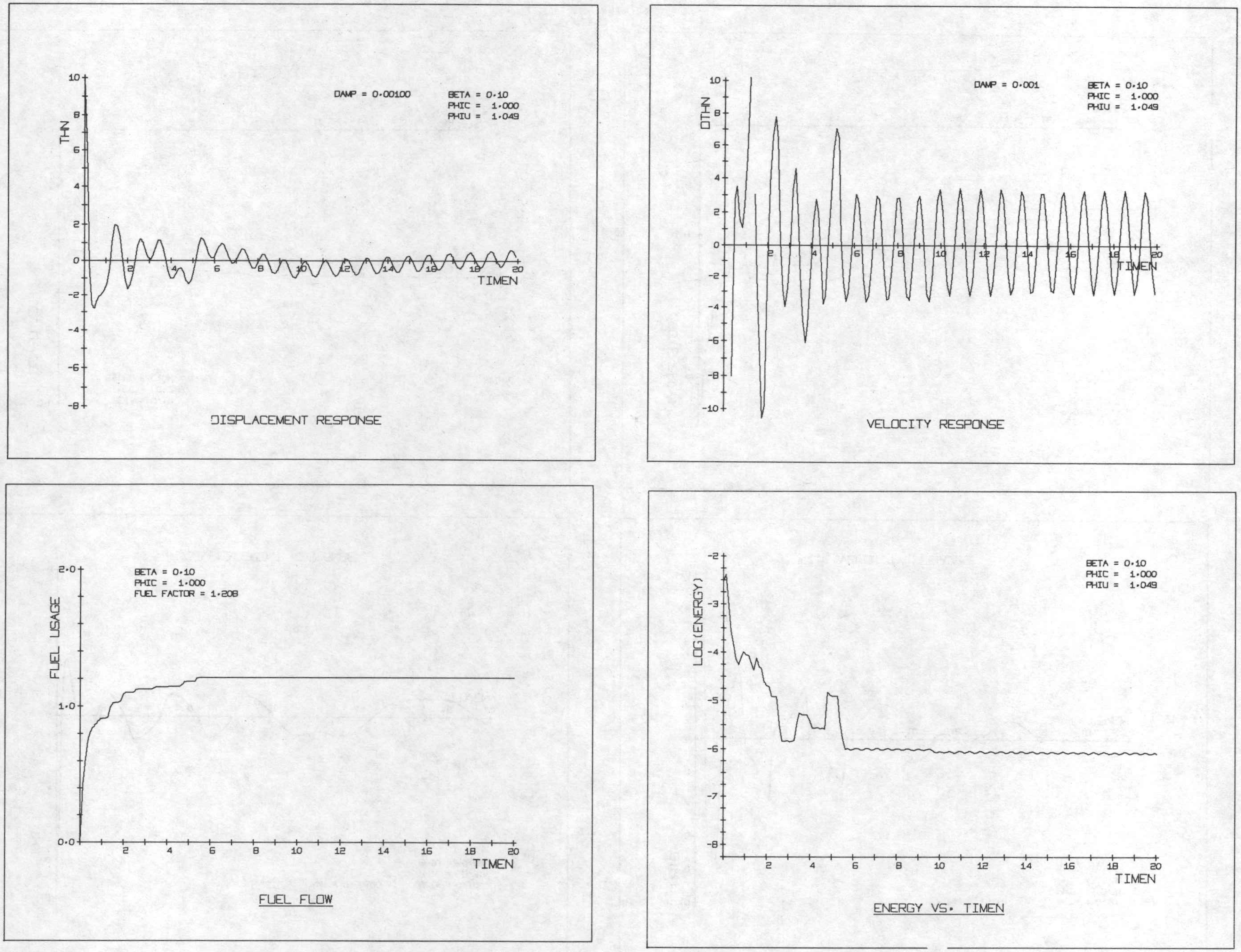

FIG. 14 SIMULATION AT BETA = 0.1, PHIC = 1.0

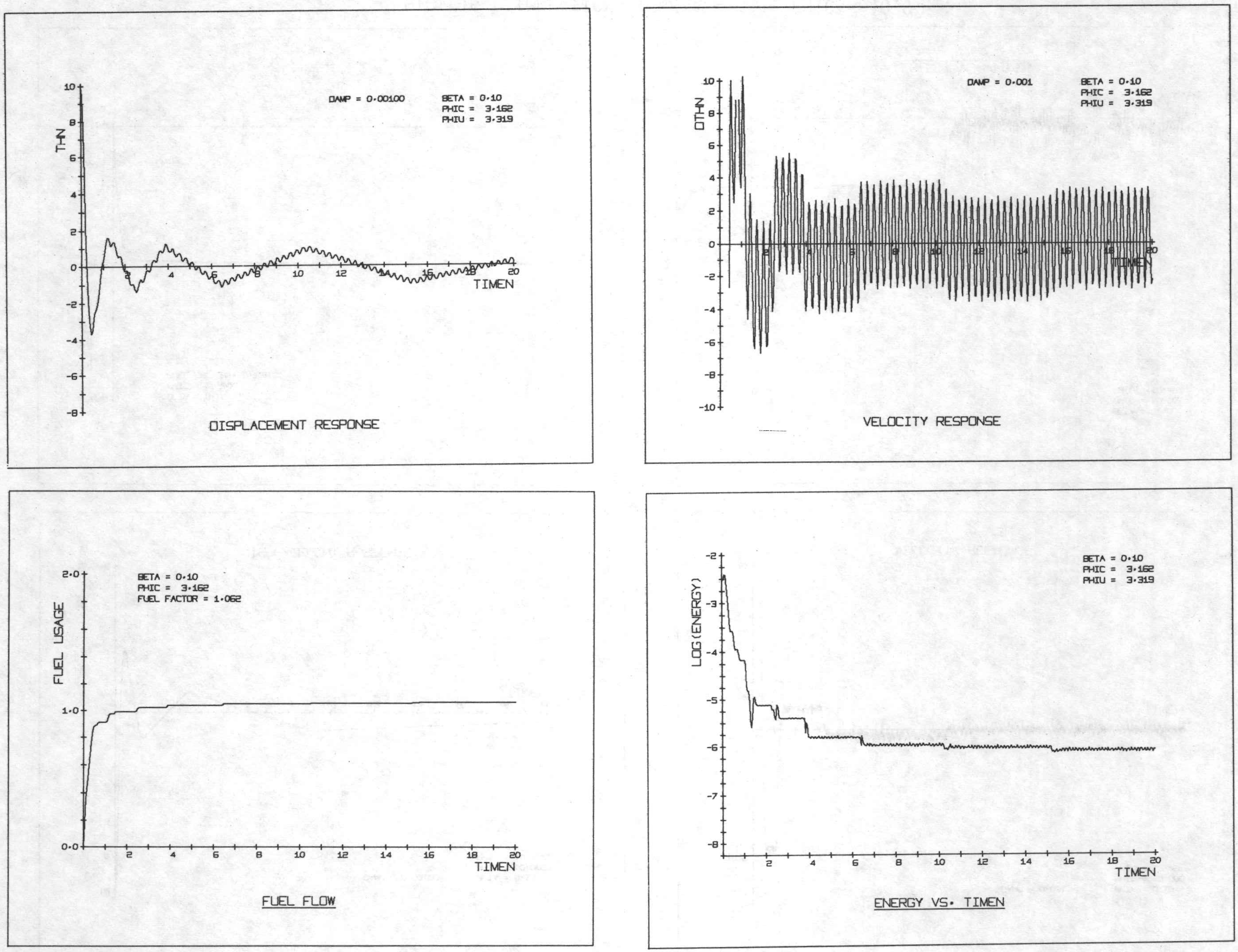

FIG. 15 SIMULATION AT BETA = 0.1, PHIC = 3.16

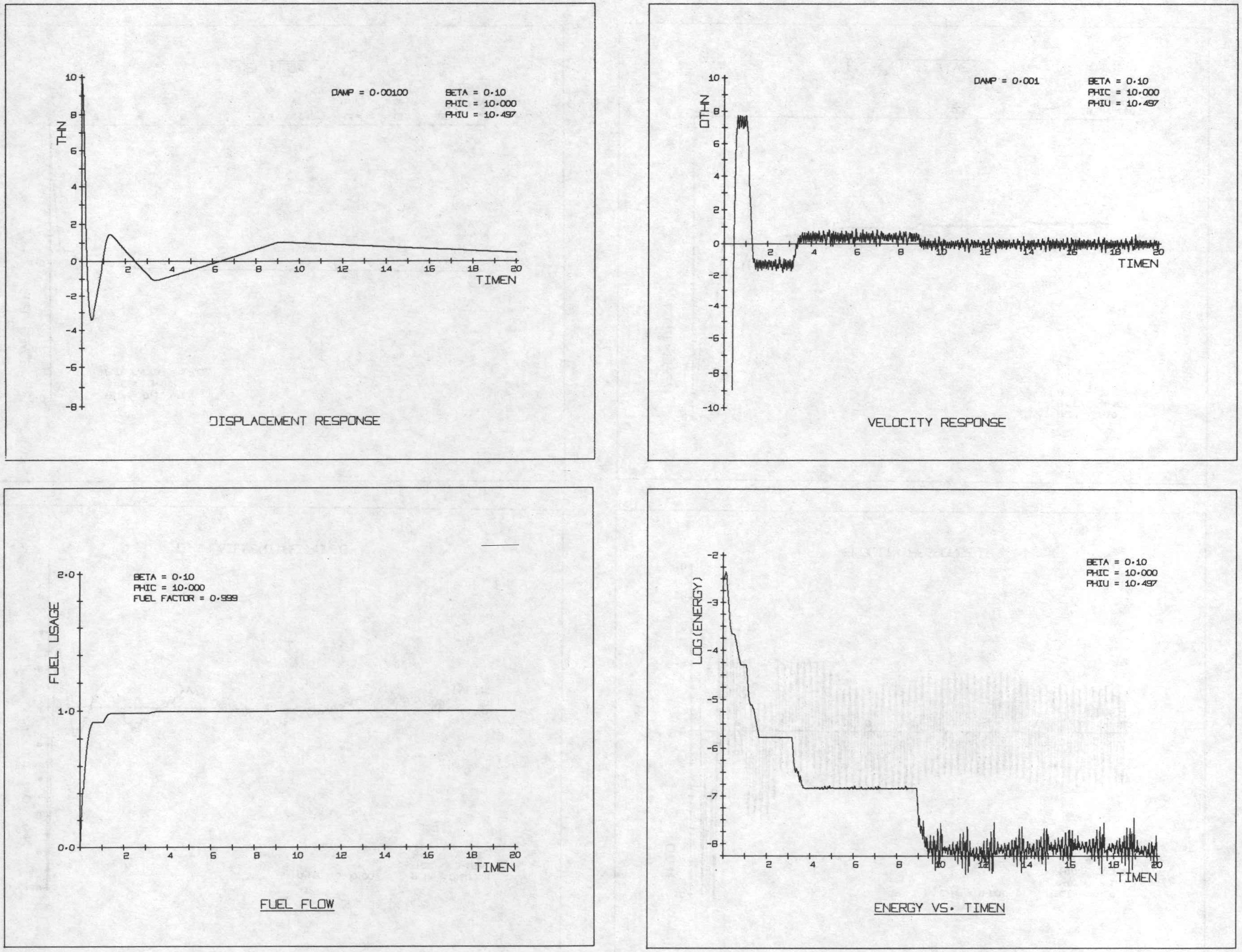

FIG. 16 SIMULATION AT BETA = 0.1, PHIC = 10.0

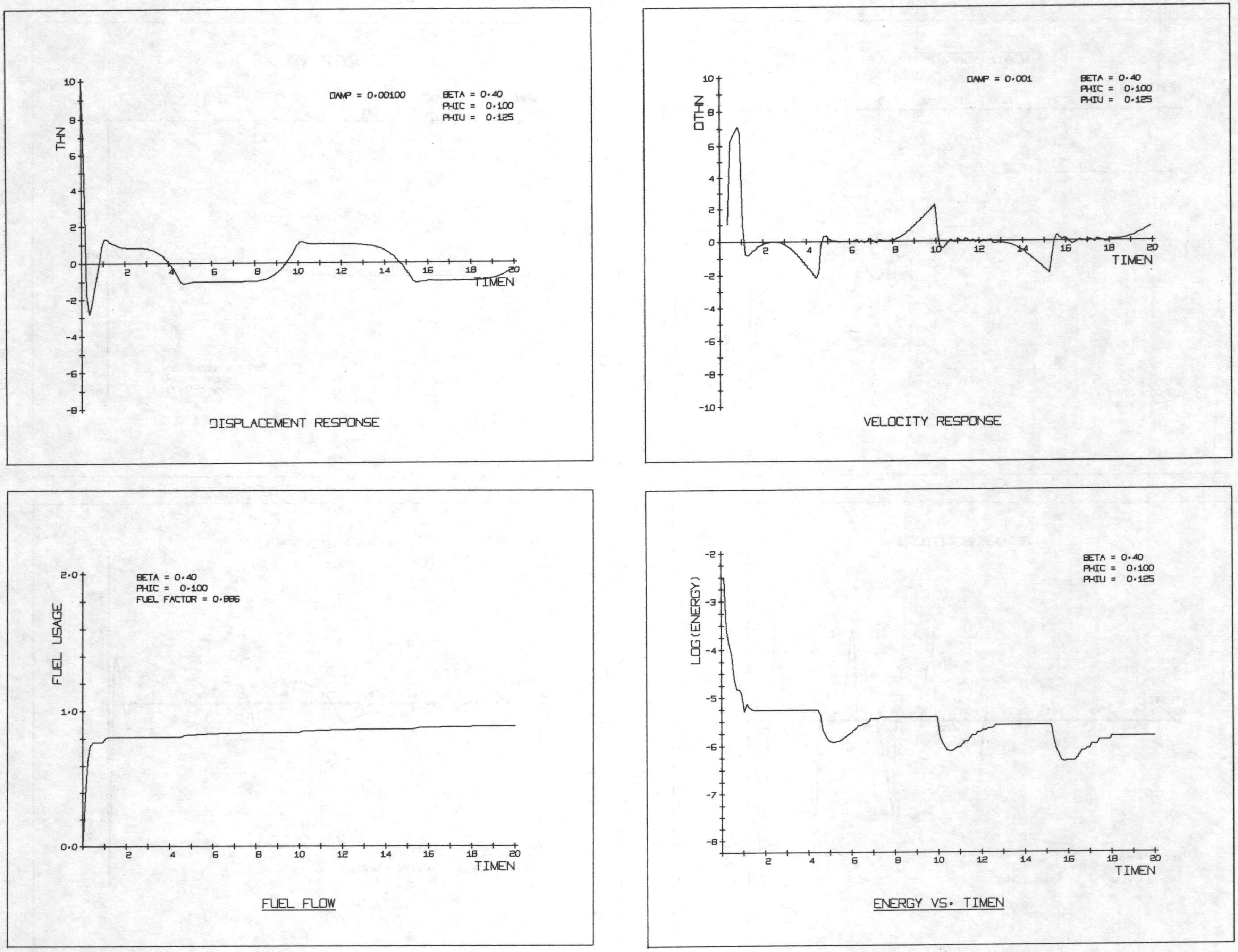

FIG. 17 SIMULATION AT BETA = 0.4, PHIC = 0.1

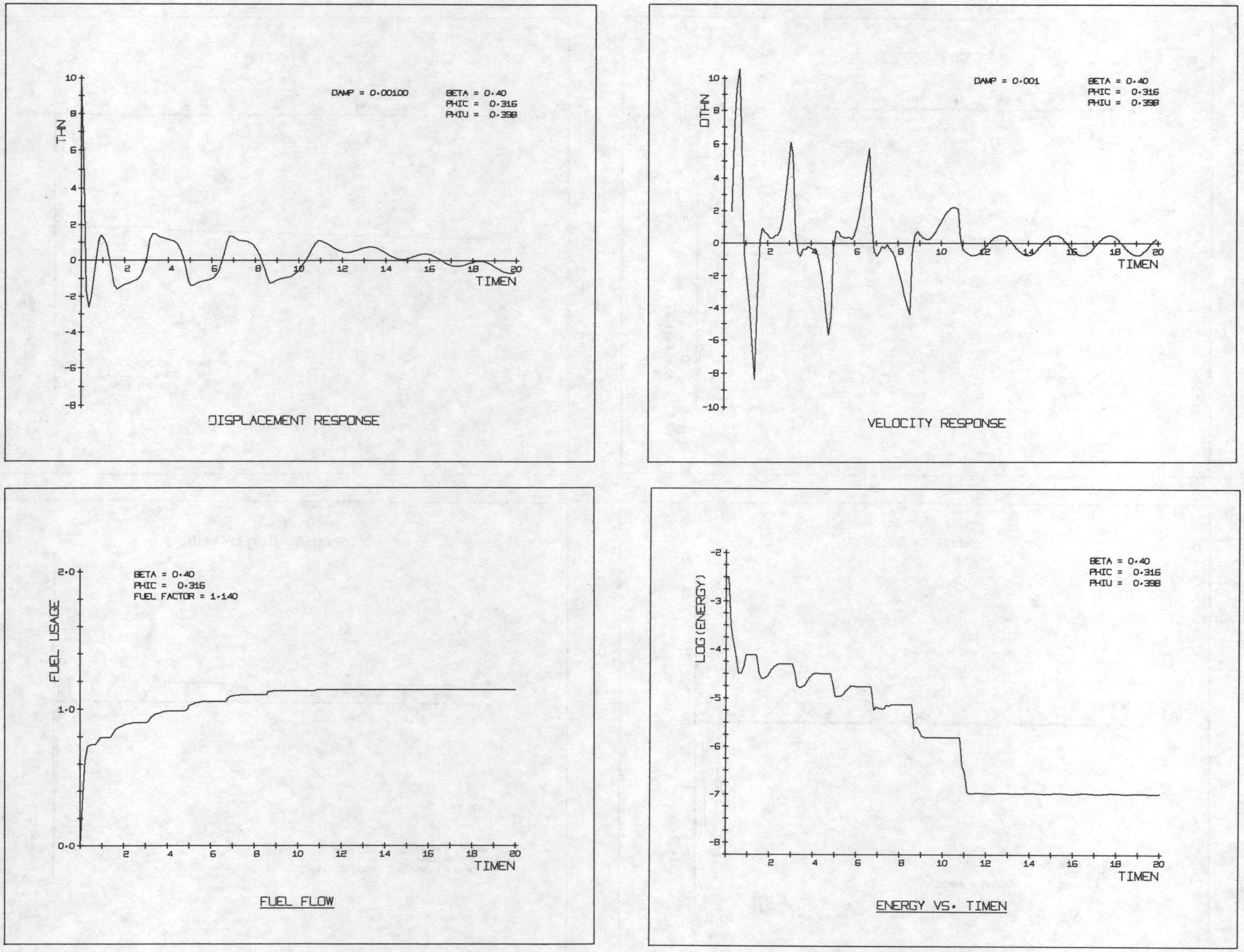

FIG. 18 SIMULATION AT BETA = 0.4, PHIC = 0.316

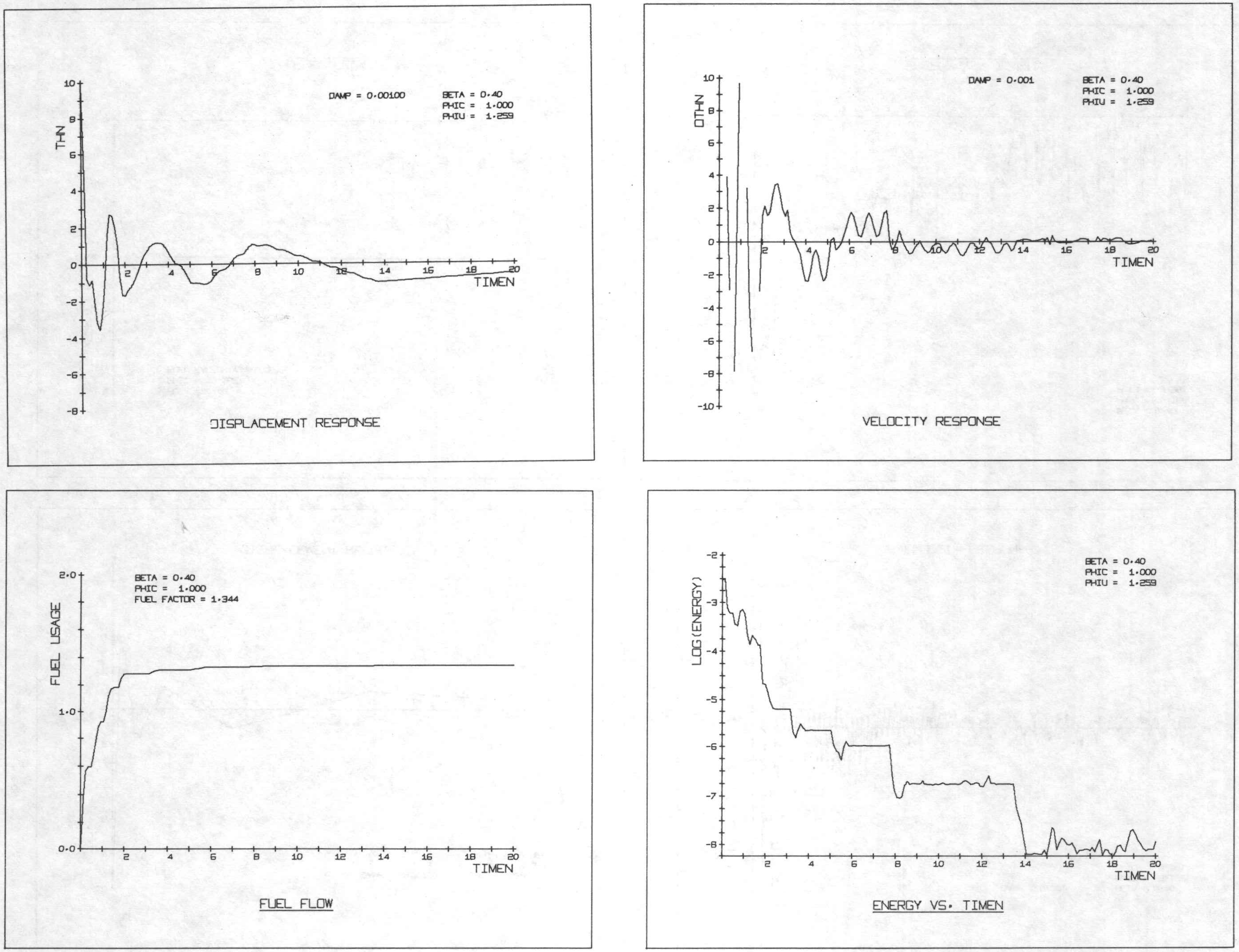

FIG. 19 SIMULATION AT BETA = 0.4, PHIC = 1.0

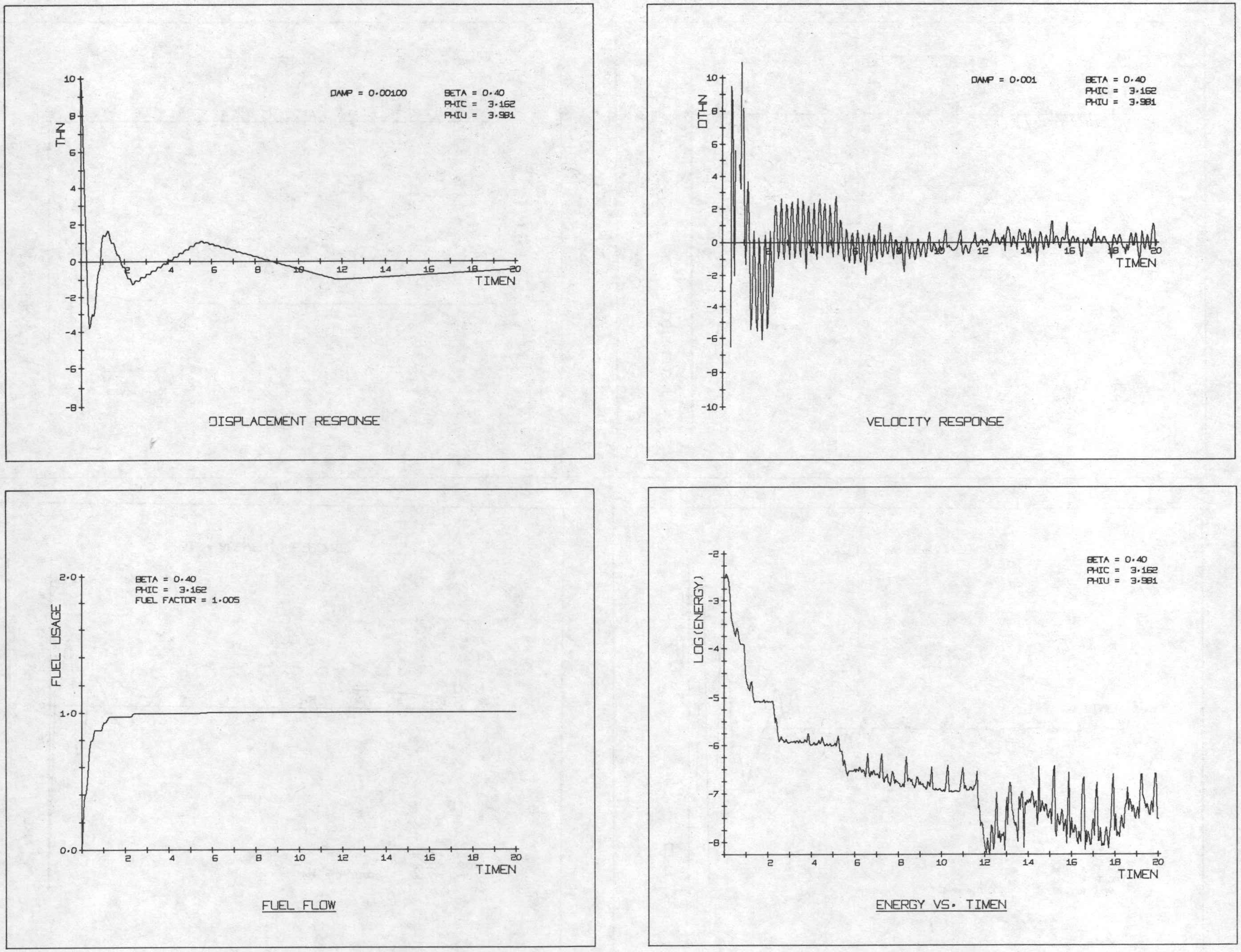

FIG. 20 SIMULATION AT BETA = 0.4, PHIC = 3.16

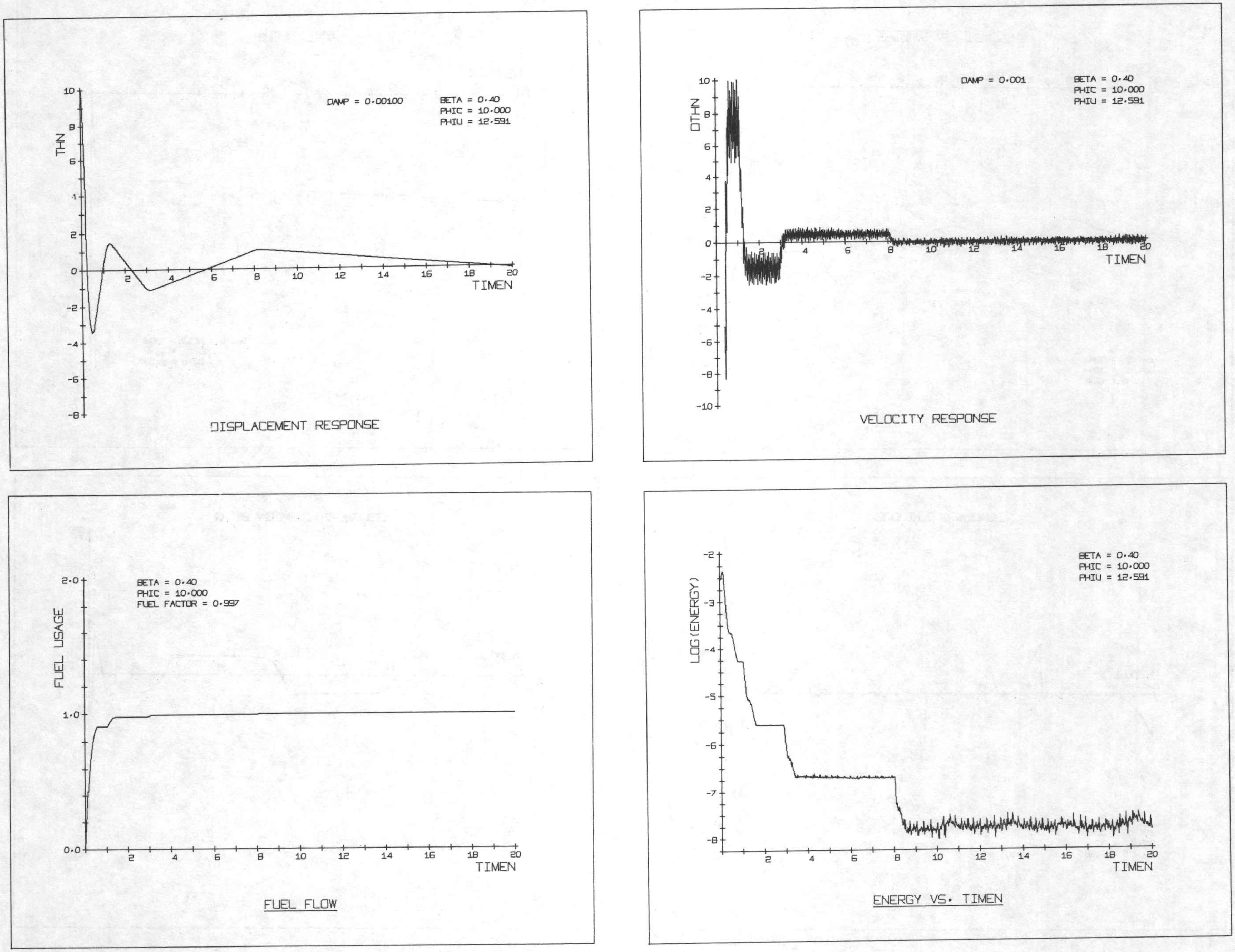

FIG. 21 SIMULATION AT BETA = 0.4, PHIC = 10.0

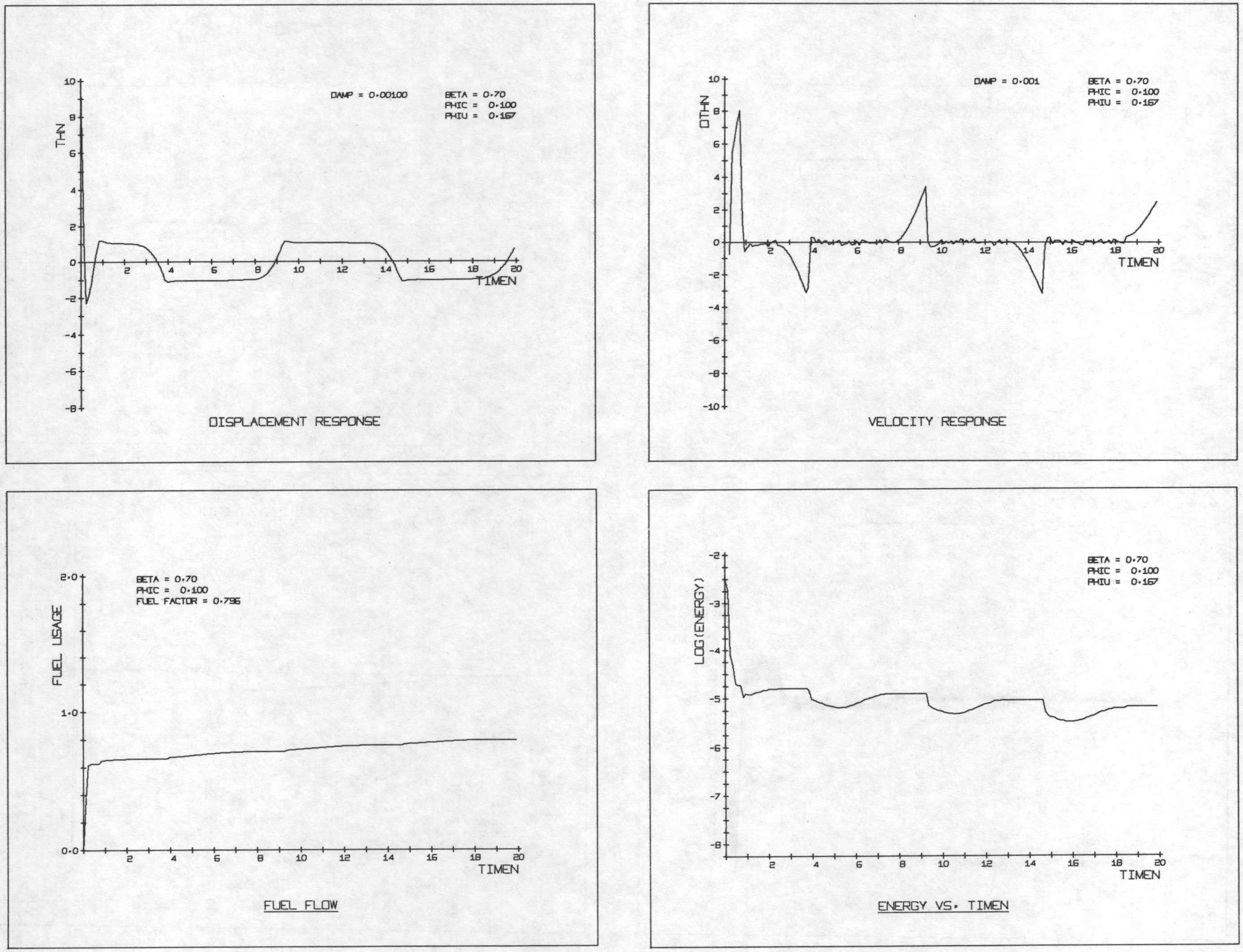

FIG. 22 SIMULATION AT BETA = 0.7, PHIC = 0.1

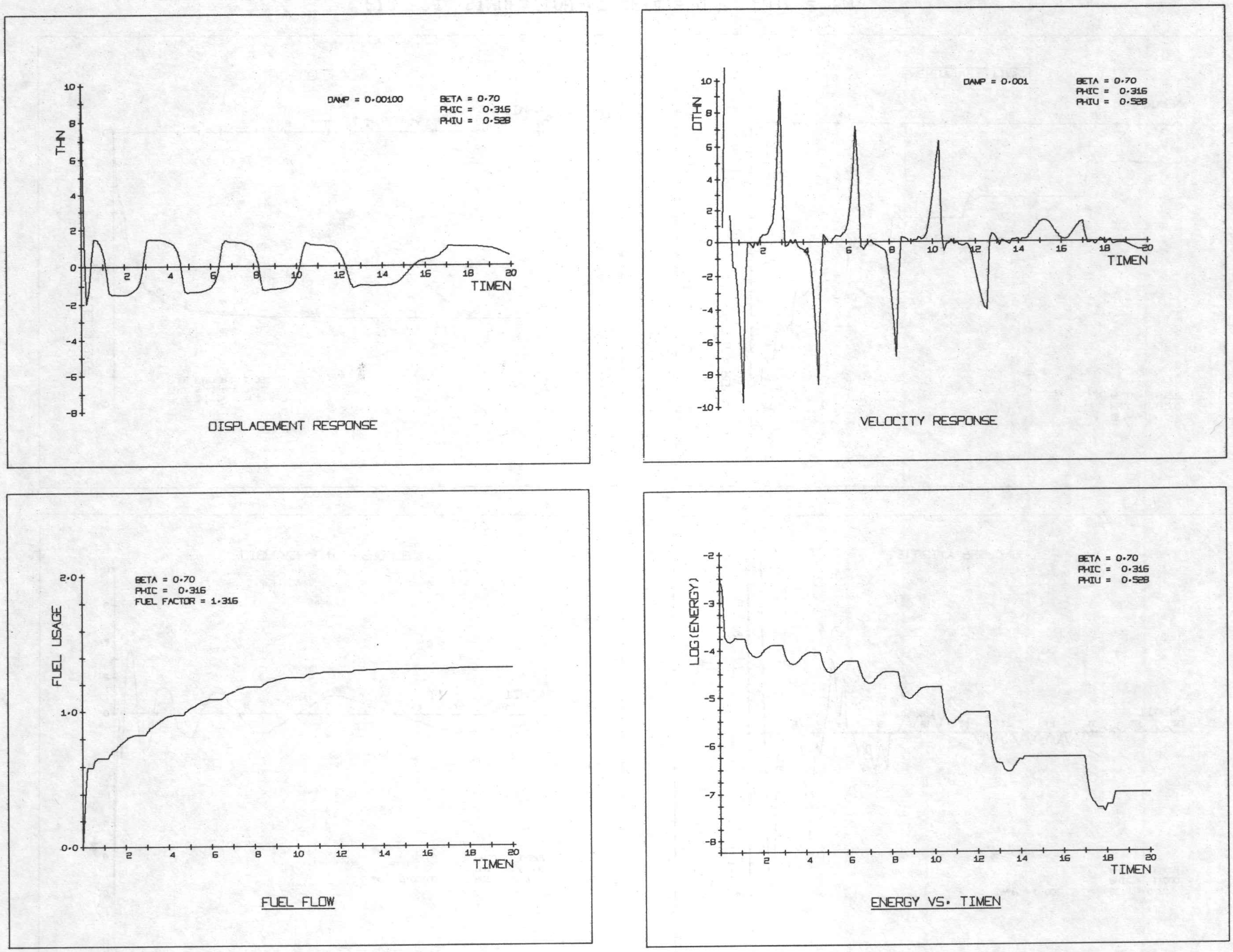

FIG. 23 SIMULATION AT BETA = 0.7, PHIC = 0.316

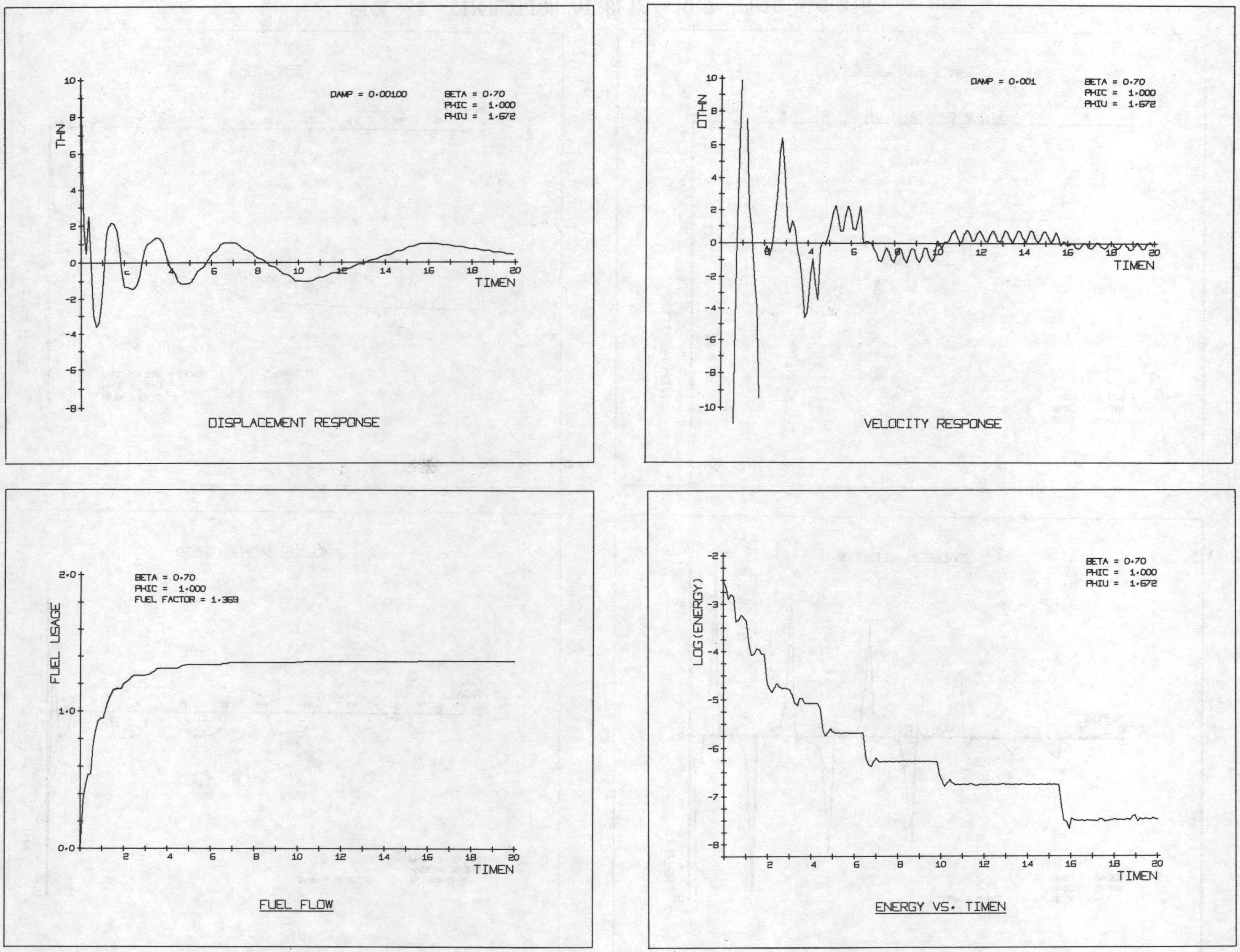

FIG. 24 SIMULATION AT BETA = 0.7, PHIC = 1.0

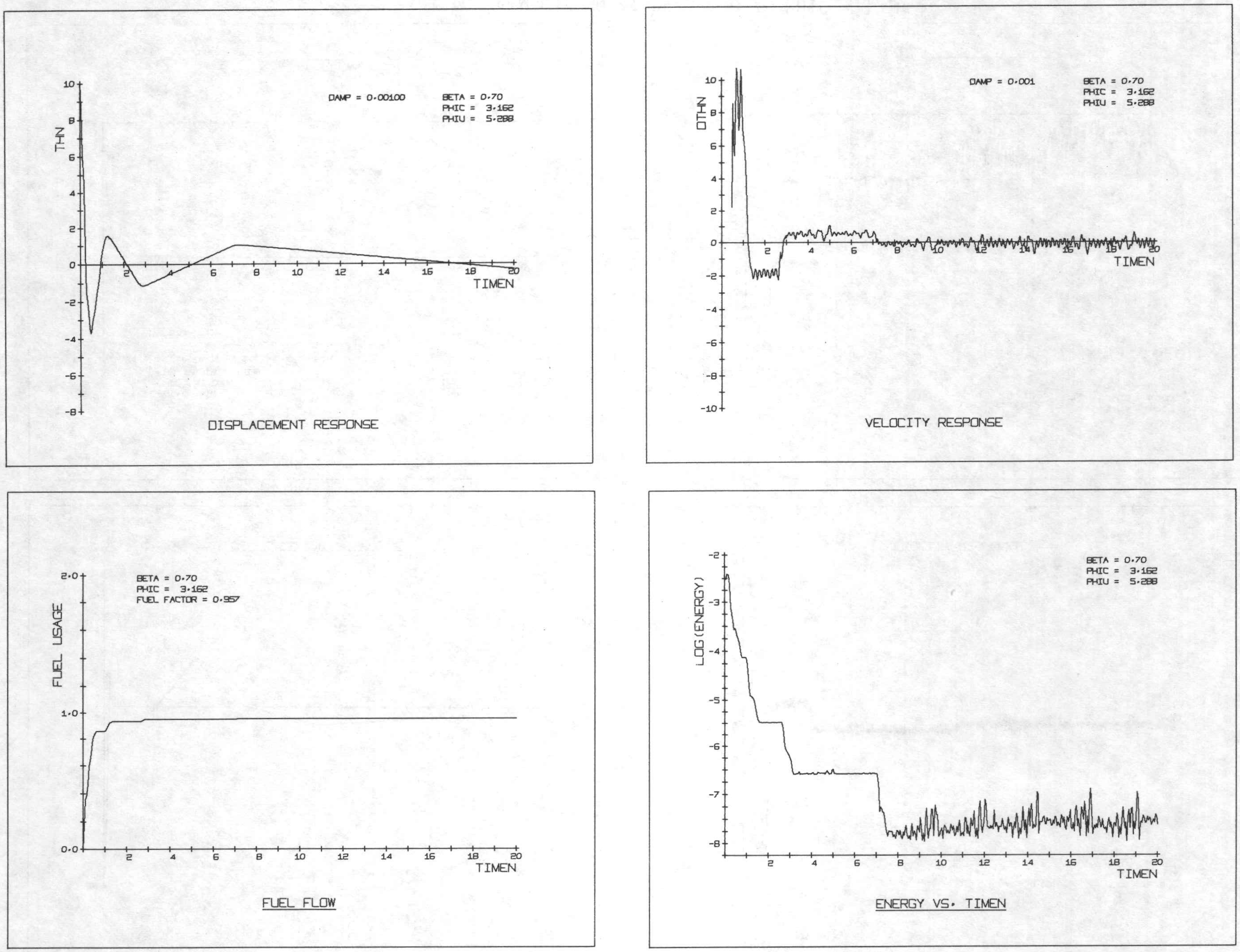

FIG. 25 SIMULATION AT BETA = 0.7, PHIC = 3.16

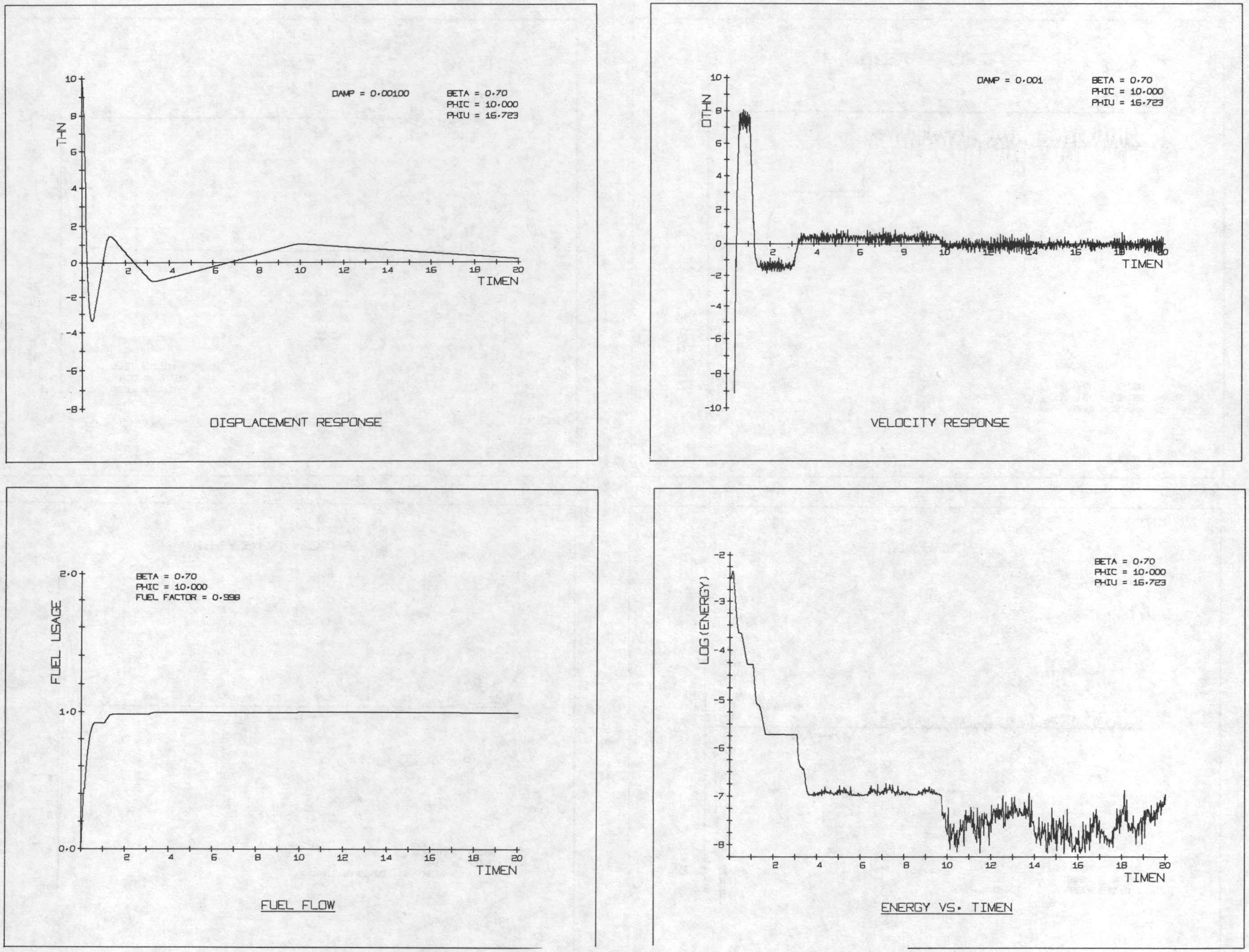

FIG. 26 SIMULATION AT BETA = 0.7, PHIC = 10.0

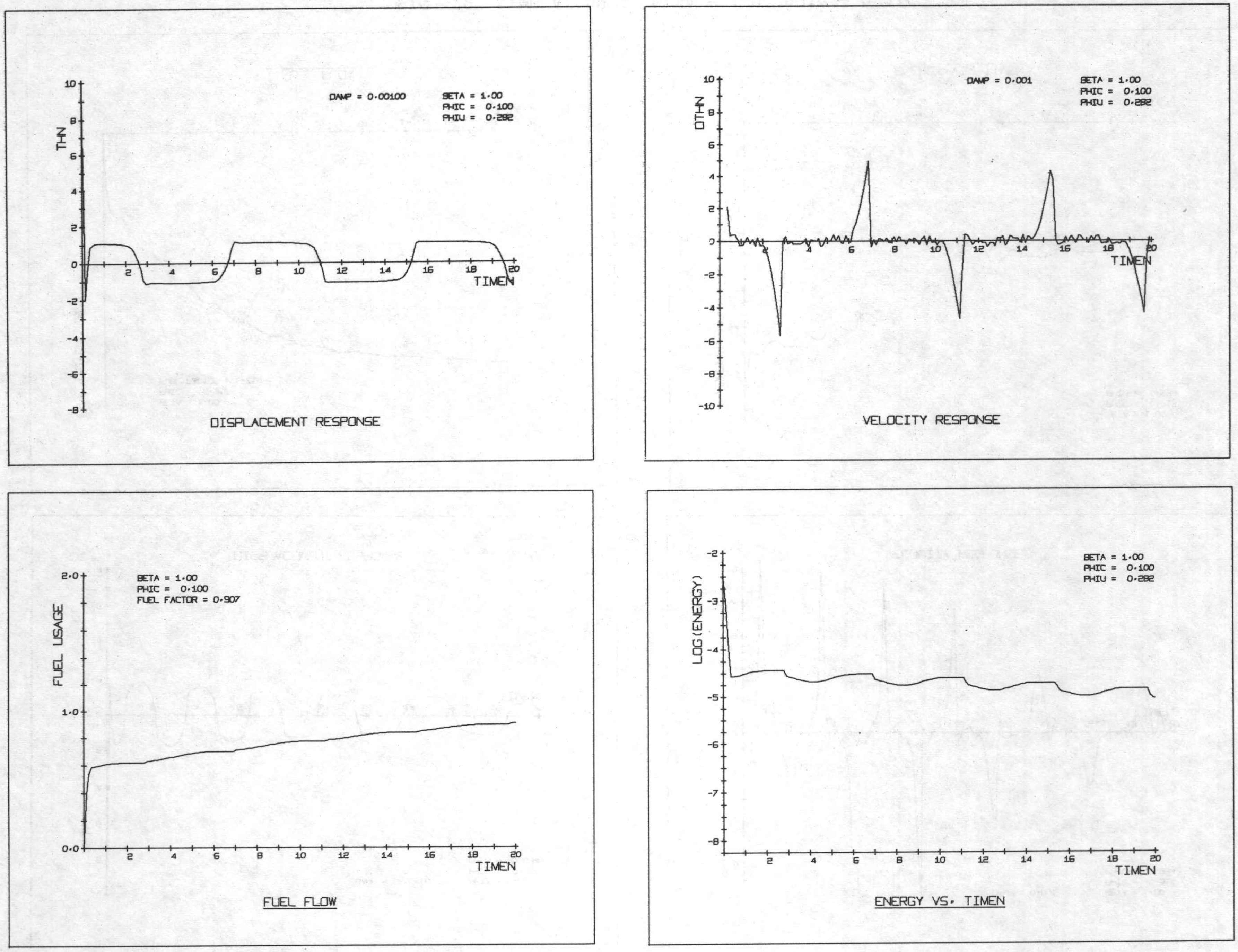

FIG. 27 SIMULATION AT BETA = 1.0, PHIC = 0.1

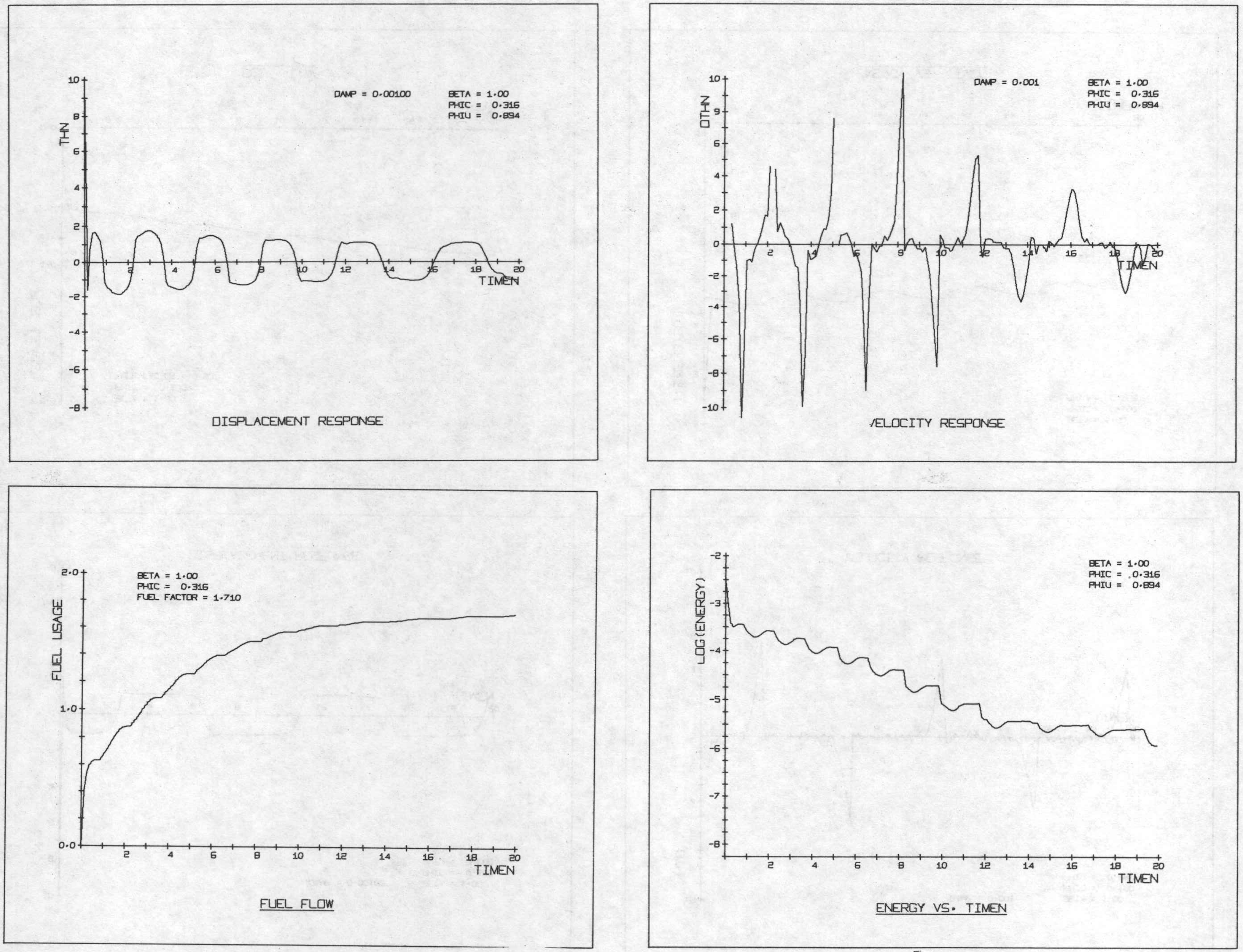

FIG. 28 SIMULATION AT BETA = 1.0, PHIC = 0.316

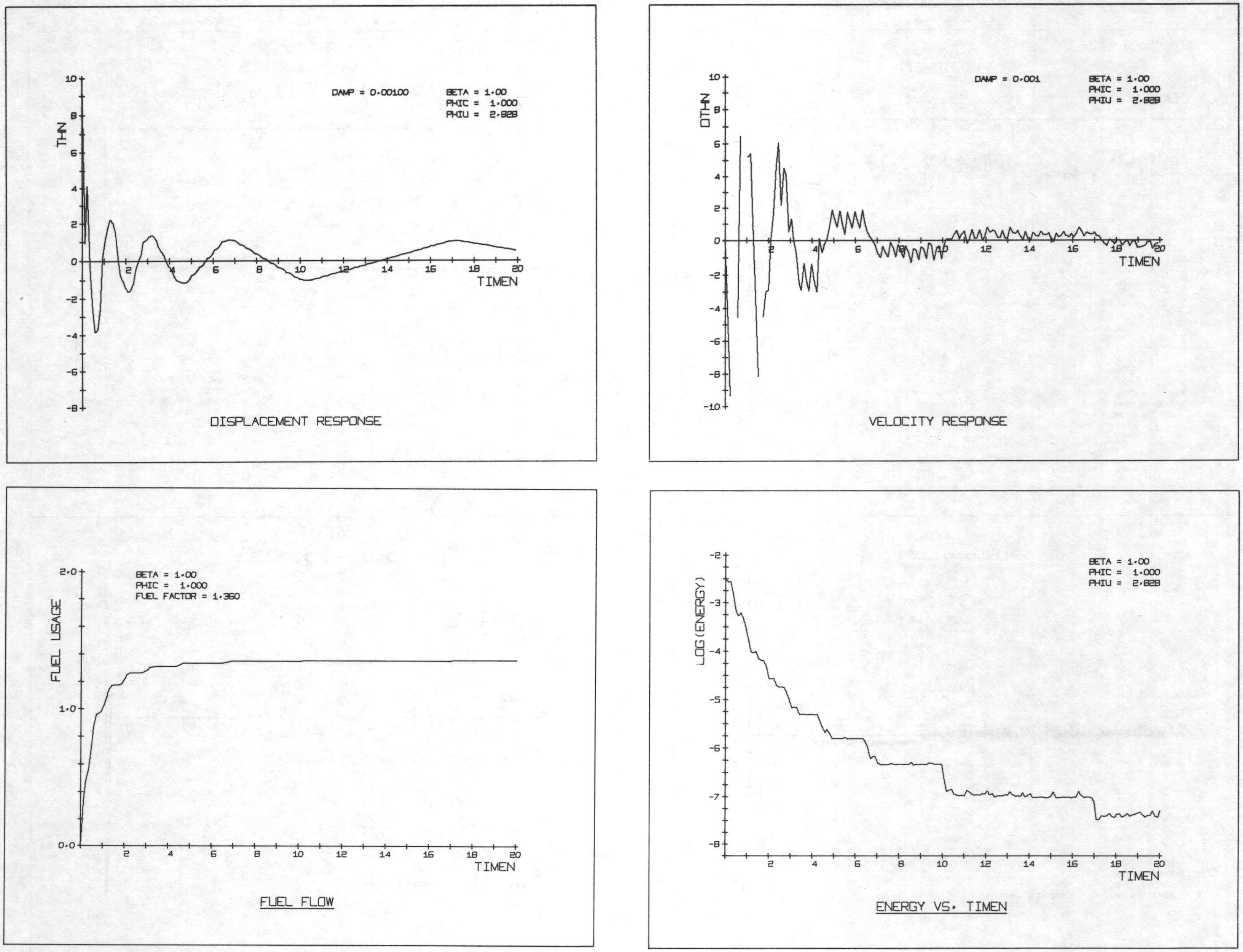

FIG. 29 SIMULATION AT BETA = 1.0, PHIC = 1.0

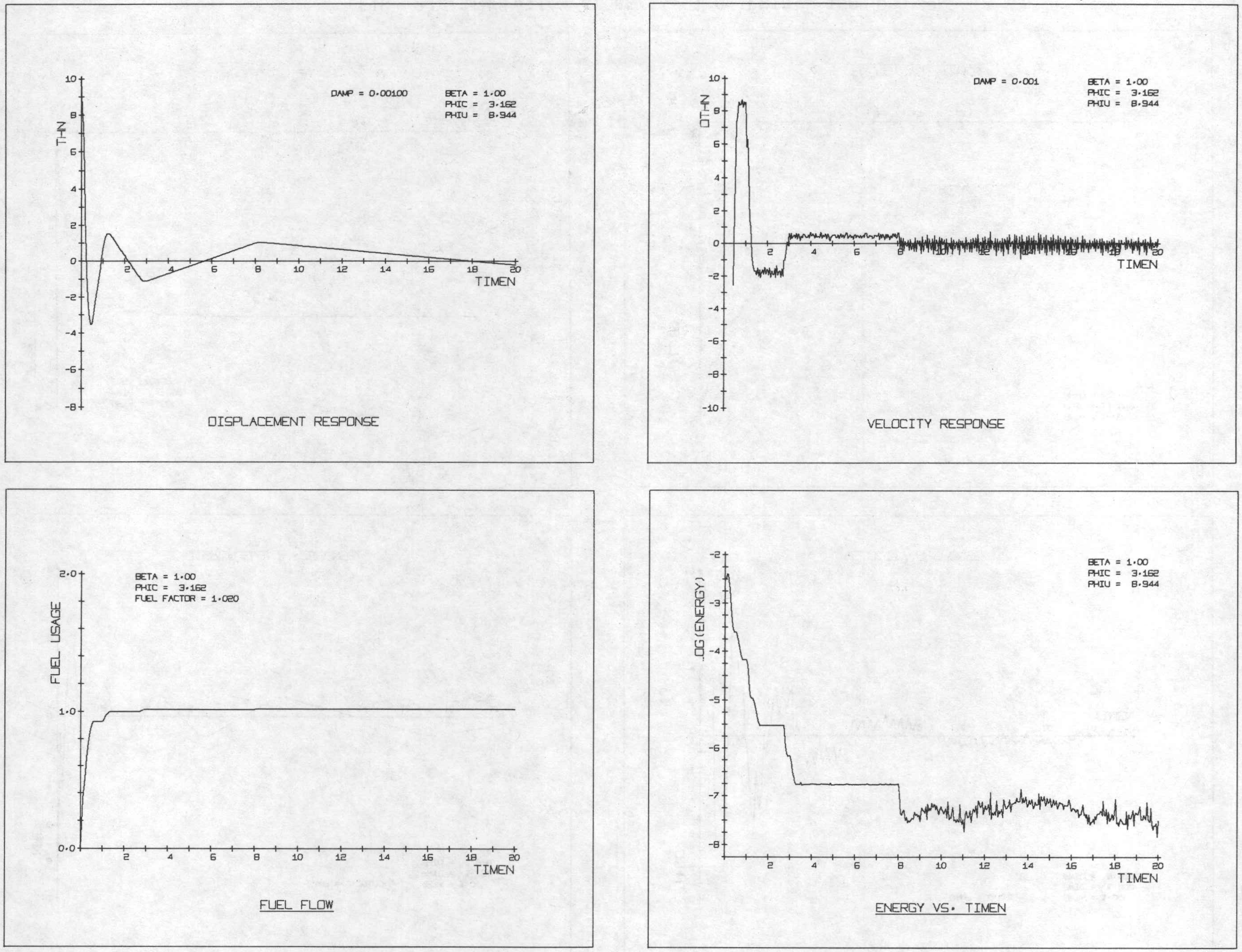

FIG. 30 SIMULATION AT BETA = 1.0, PHIC = 3.16

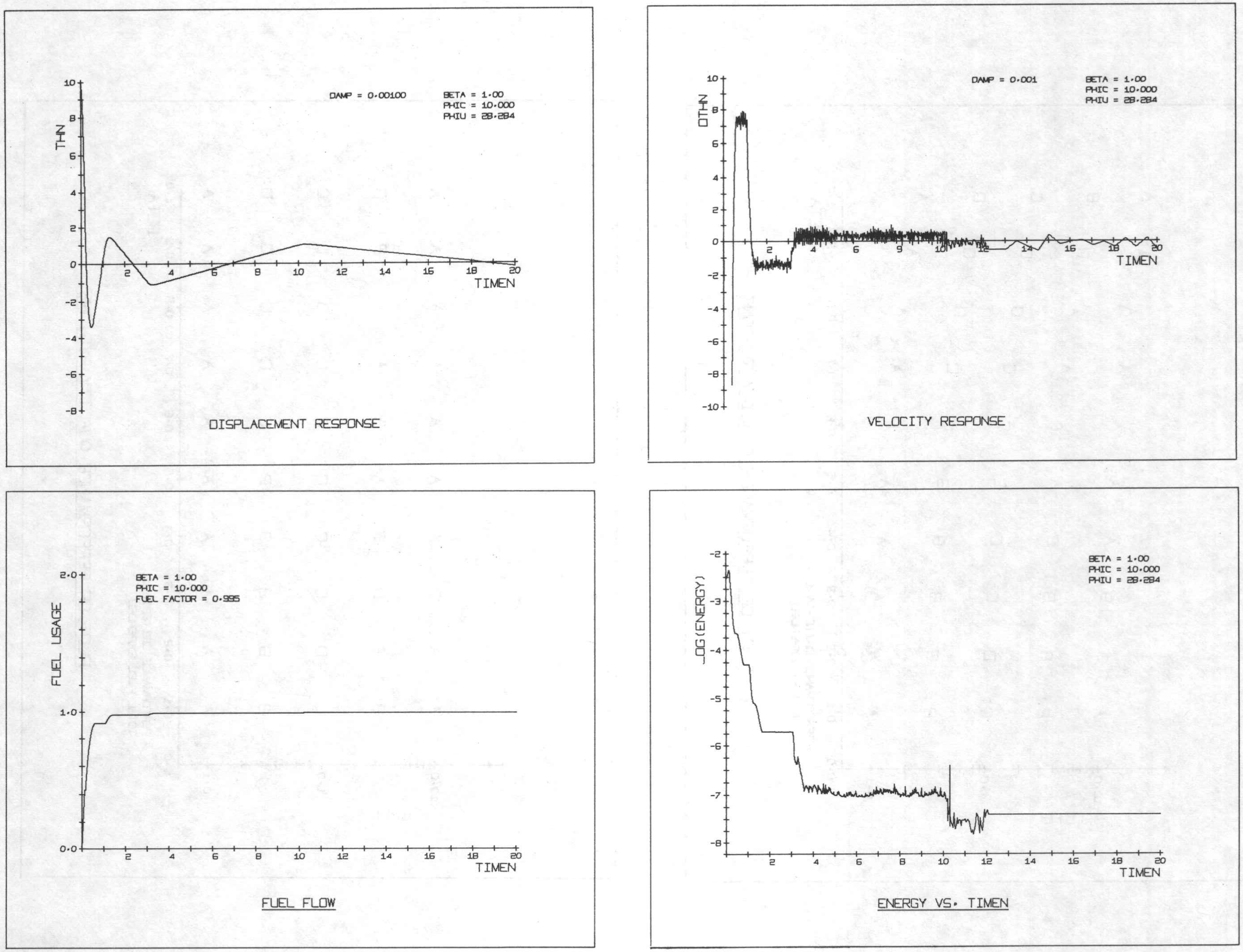

FIG. 31 SIMULATION AT BETA = 1.0, PHIC = 10.0

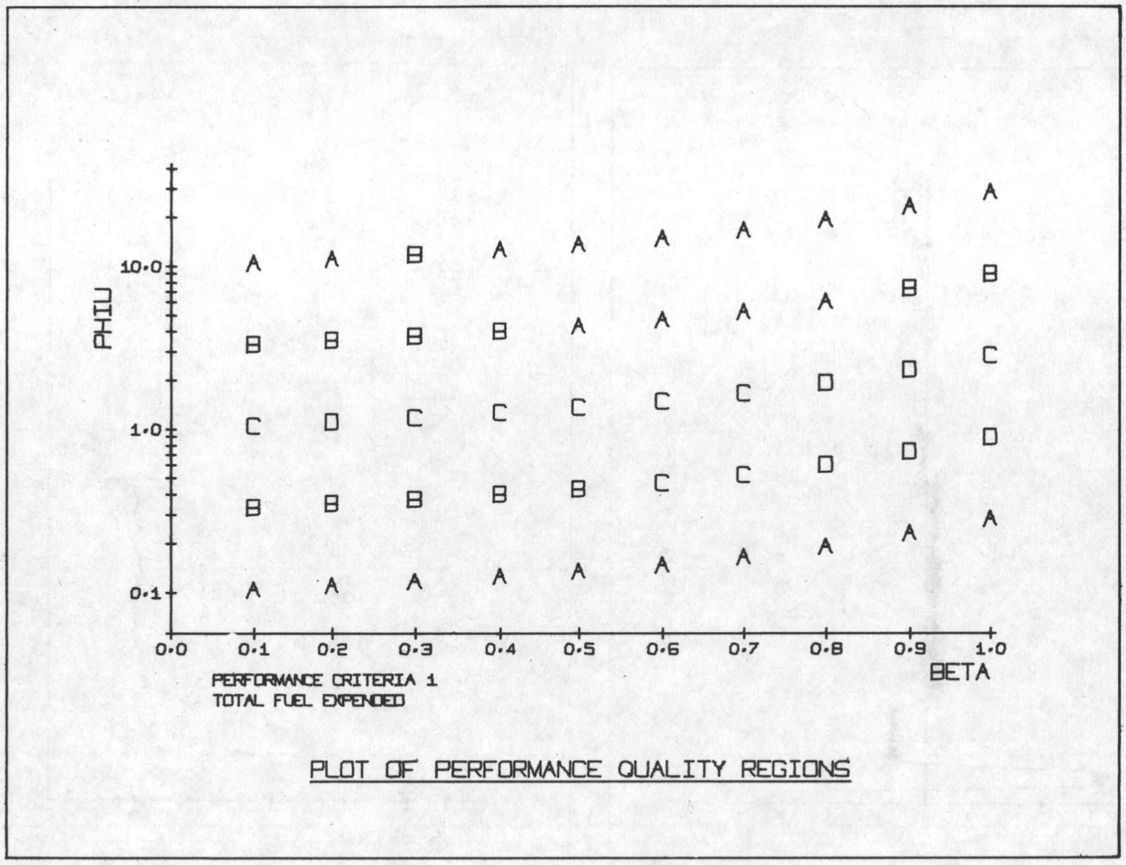

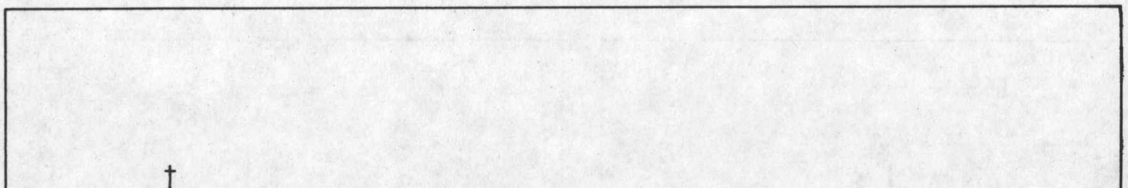

FIG. 32 PERFORMANCE SUMMARY - CRIT. 1

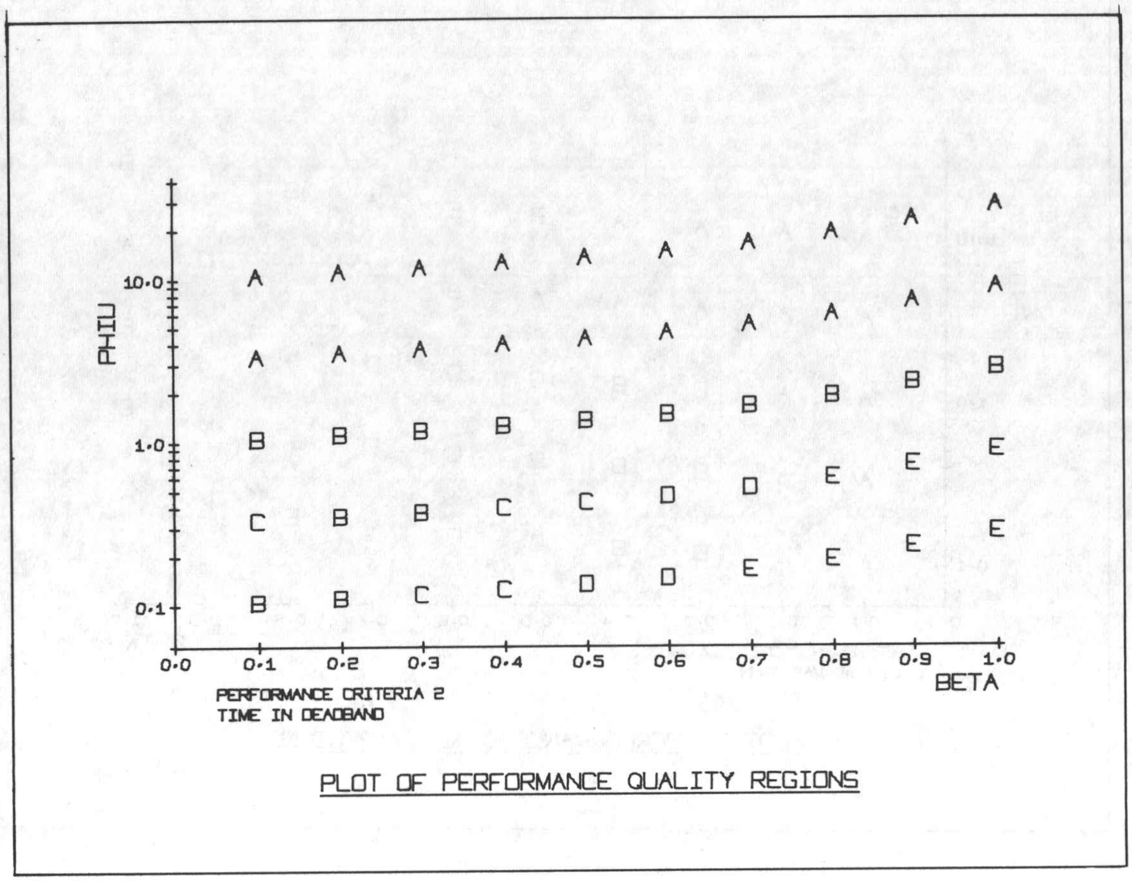

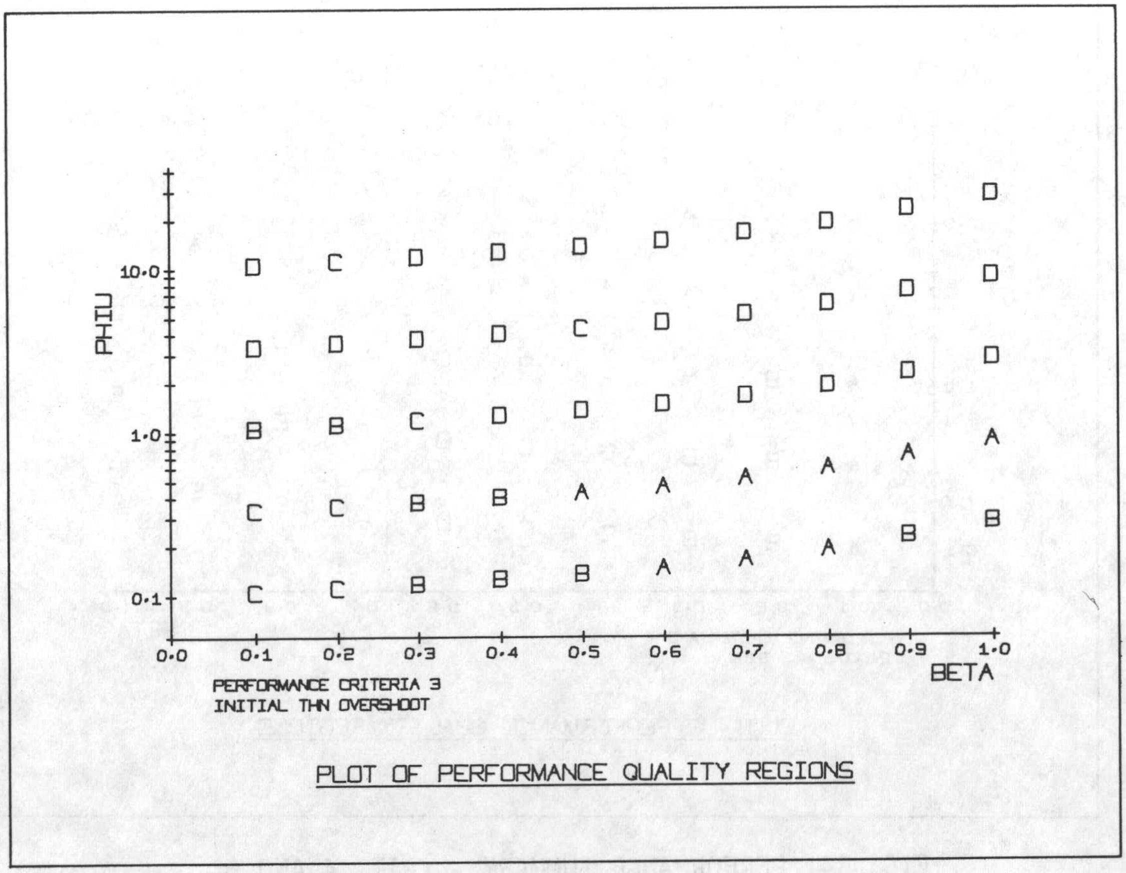

FIG. 33 PERFORMANCE SUMMARY - CRIT. 2 AND 3

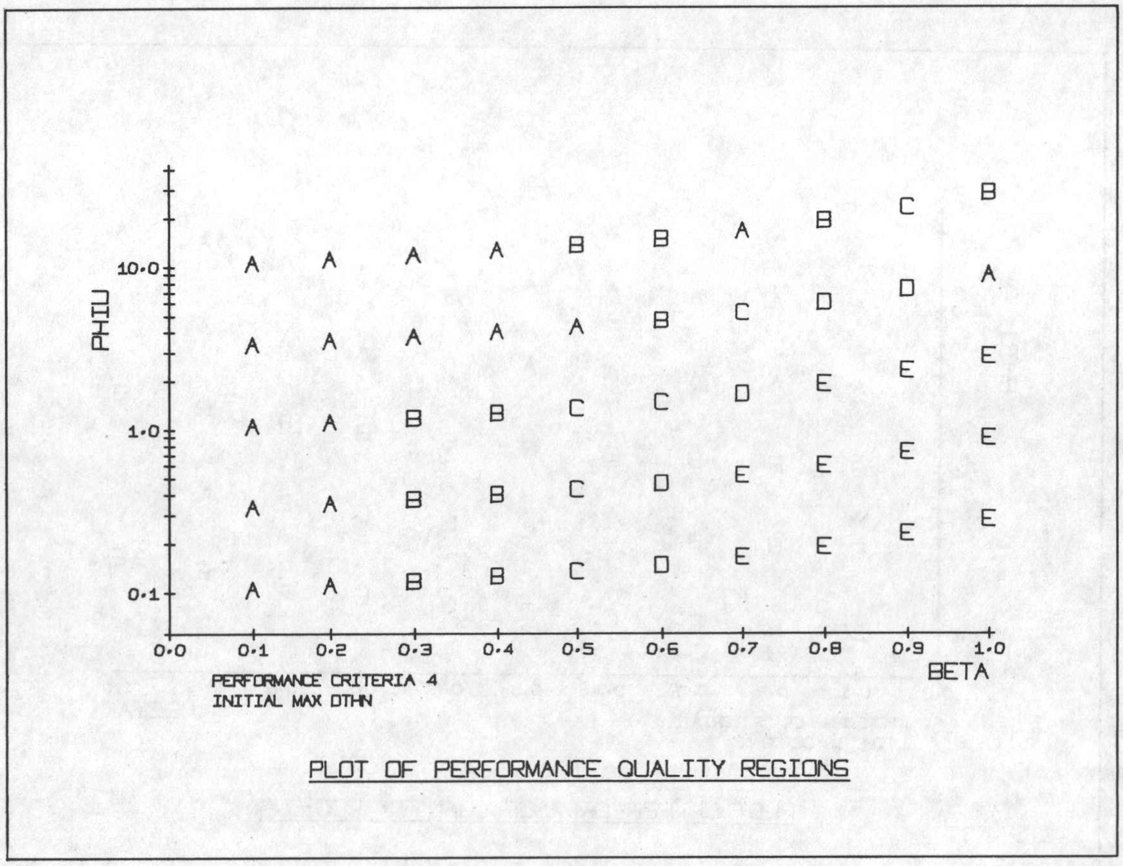

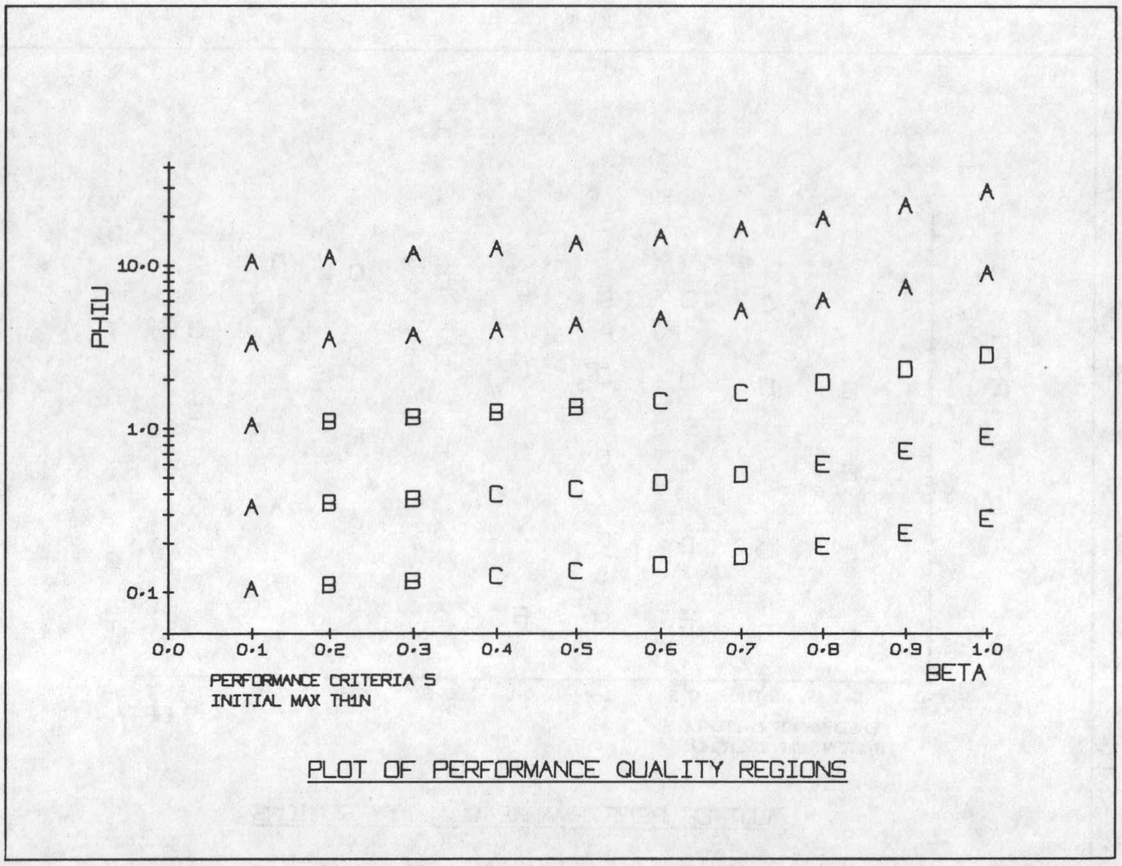

FIG. 34 PERFORMANCE SUMMARY - CRIT. 4 AND 5

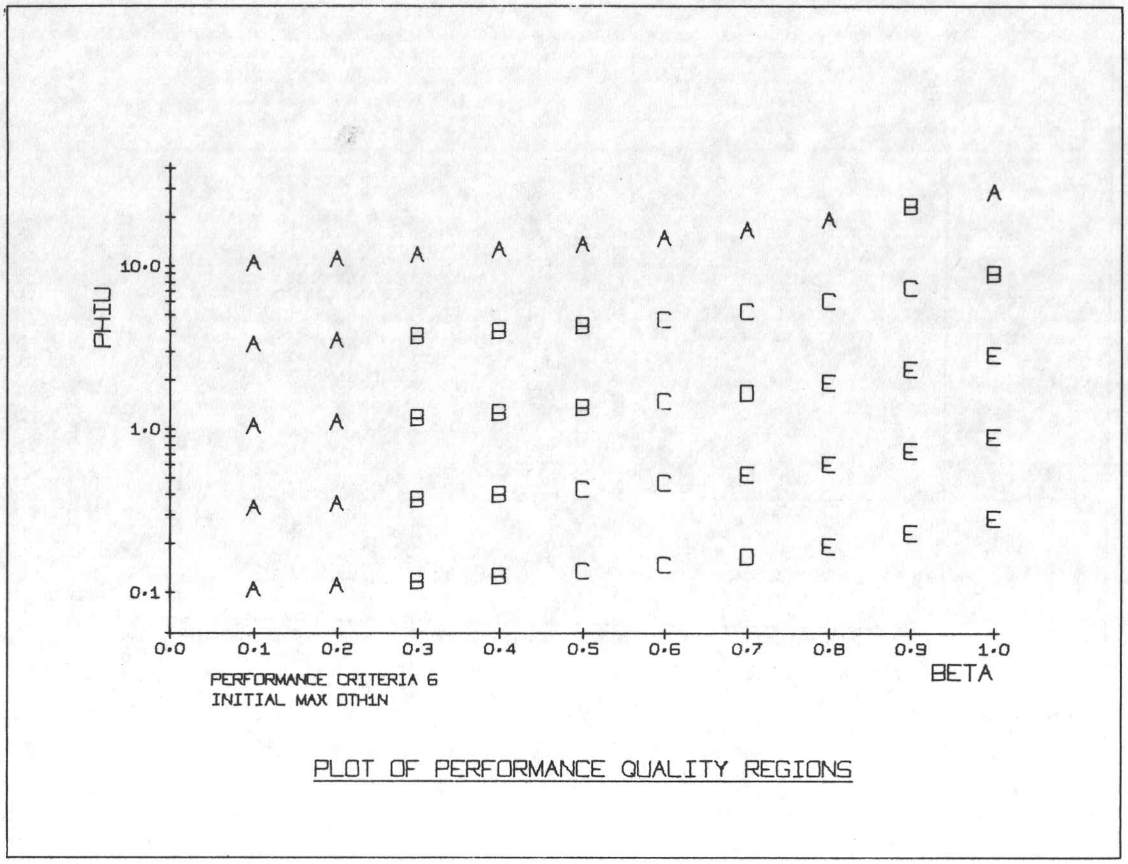

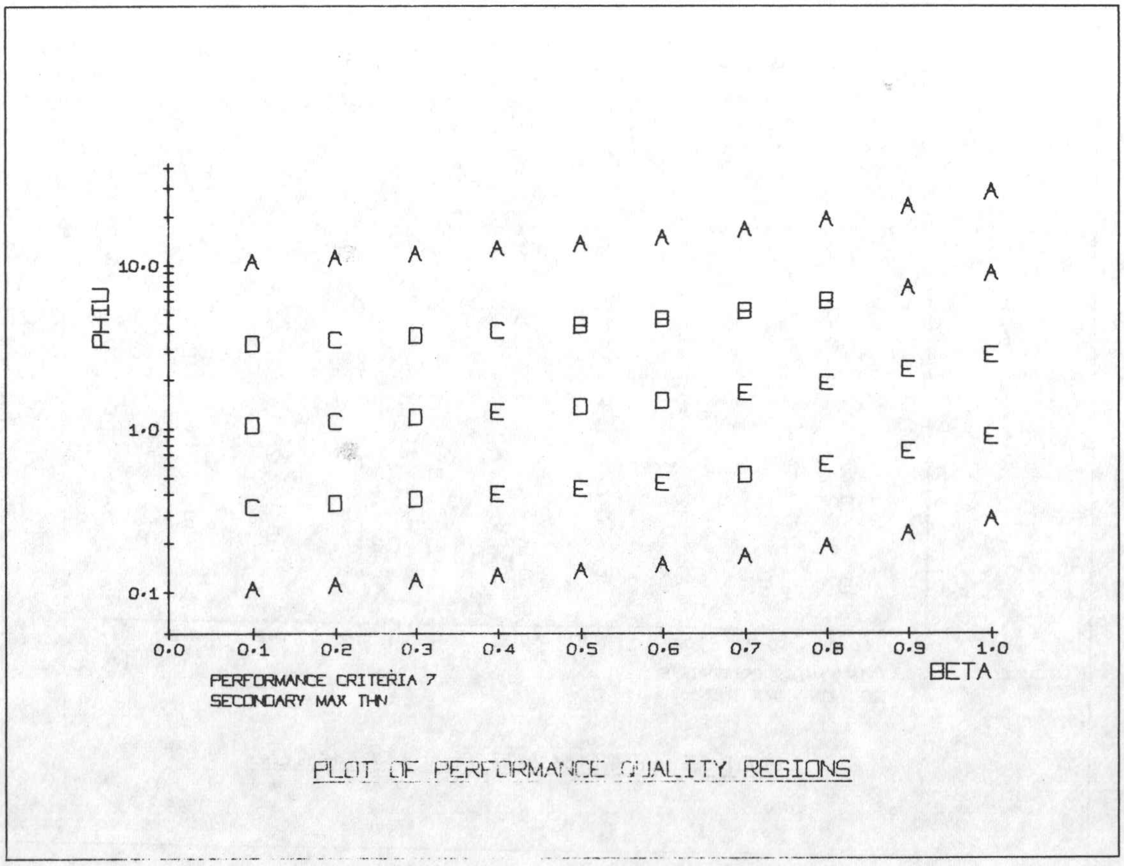

FIG. 35 PERFORMANCE SUMMARY - CRIT. 6 AND 7

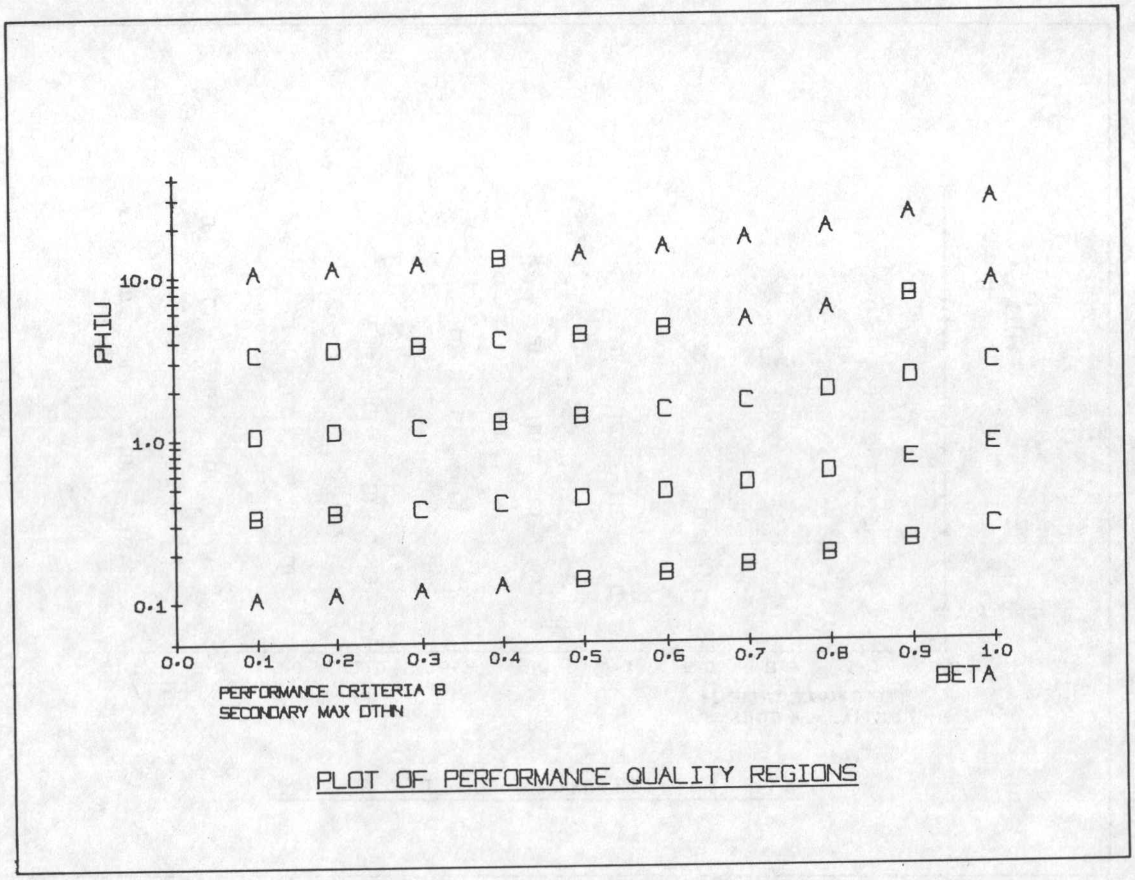

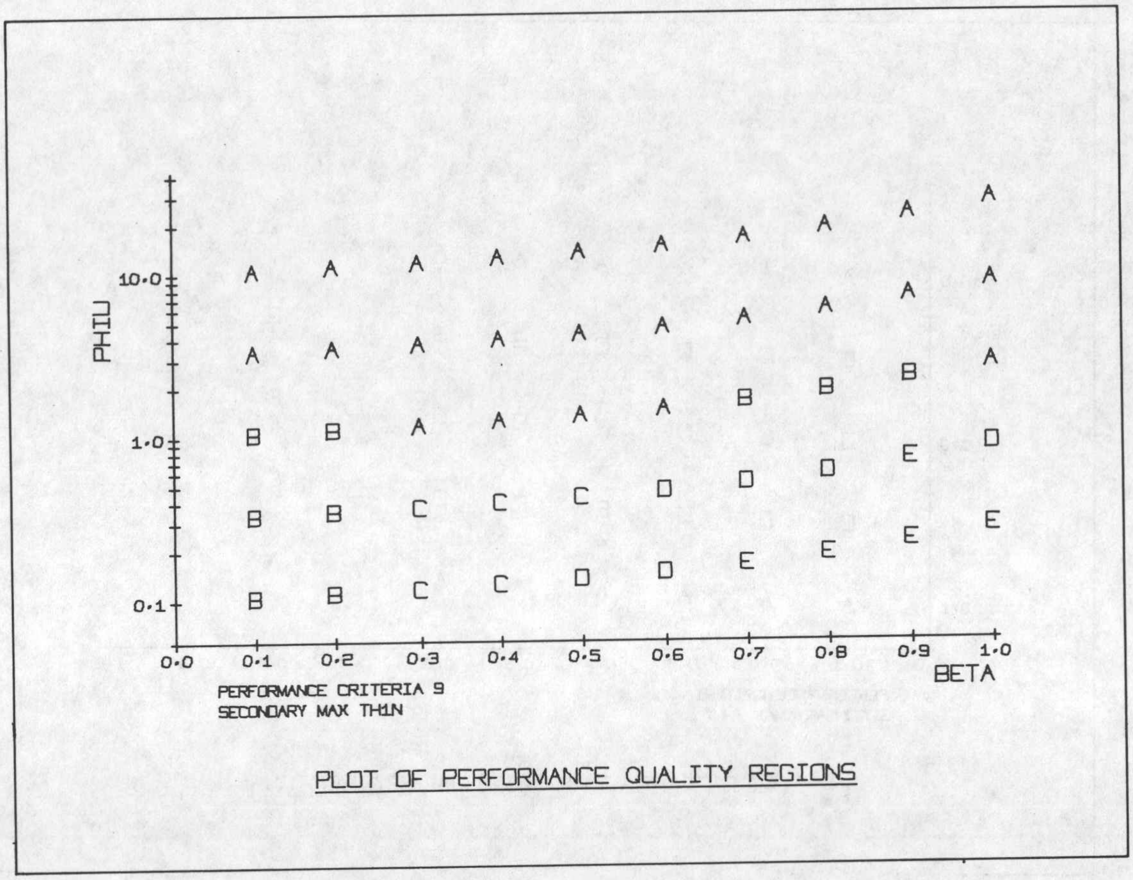

FIG. 36 PERFORMANCE SUMMARY - CRIT. 8 AND 9

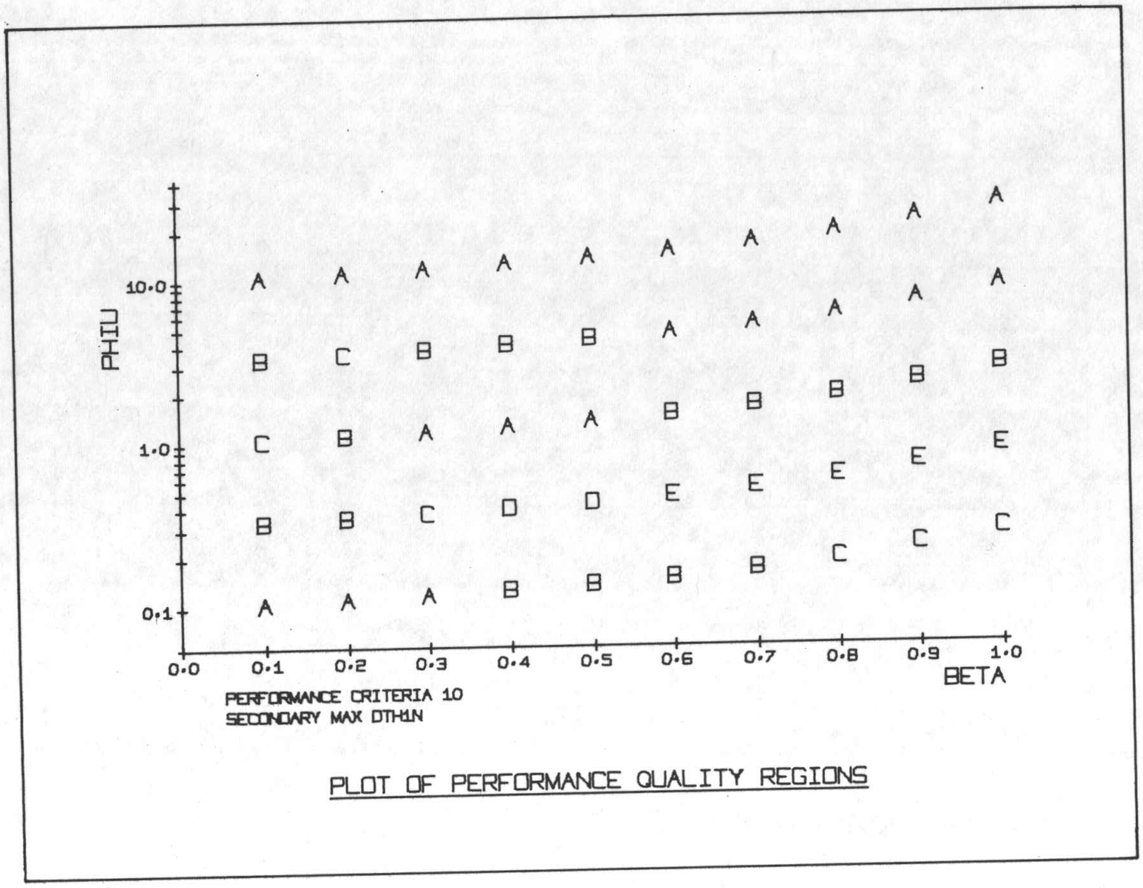

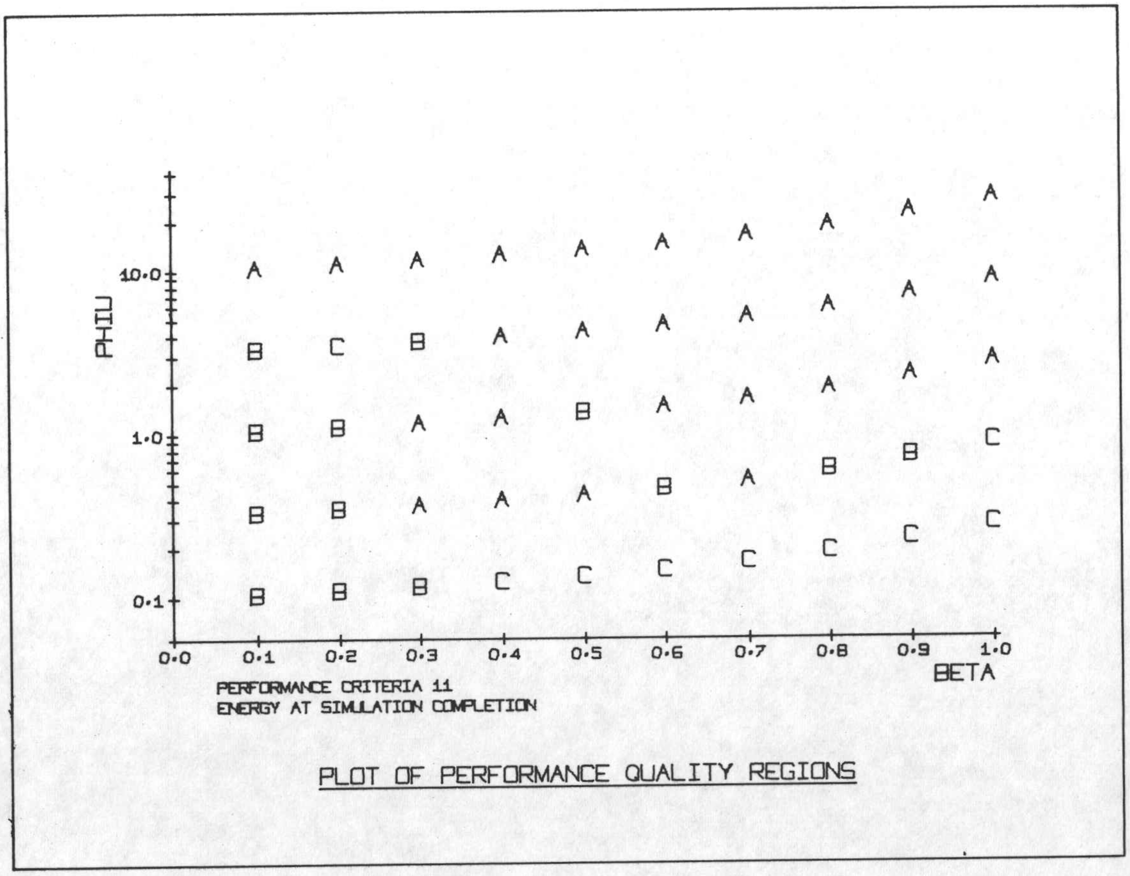

FIG. 37 PERFORMANCE SUMMARY - CRIT. 10 AND 11

APPENDIX A

This appendix contains a computer listing for the following programs:

(i) CSMP simulation program

(ii) Program "SIGVALS"

(iii) Program to calculate and plot performance quality regions

APPENDIX A COMPUTER PROGRAMS

```
******************************************************************************
     THE FOLLOWING IS PROGRAM PERFLEX, THE CSMP SIMULATION OF THE CONTROL LOOP--
******************************************************************************

//  1181,FIAH,0030,0030,1000),'PERFLEX//MALICH',MSGLEVEL=(2,0),CLASS=A
/*PRIORITY     4
//    EXEC CSMP360
//CSMP.SYSIN DD *
*  PROGRAM 'PERFLEX'  --  GUNTER MALICH

*  PERFORMANCE SIMULATION OF PSEUDO-RATE LOOP
*  ONE UNCONSTRAINED FLEXIBLE MODE INCLUDED

HISTORY RELAY(1)

INITIAL

*  SET PARAMETERS FOR FLEXIBLE BLOCK
PARAM BETA=1.0, PHIC=10.000000, PHIU=28.2845
PARAM K1C=0.925624E+00, K1U=0.374774E+01
PARAM DAMP=0.001

*  SET PARAMETERS OF CONTROL SYSTEM
PARAM KTHETA=163., H=0.0188, DB=6.10865E-03
PARAM KF=13.3, TAUF=8.8
PARAM KJET=0.12, IRIG=68.

*  SET EXTERNAL INPUTS
PARAM THIN=0.0
PARAM TD=0.0

*  SET INITIAL CONDITIONS
INCON THRON=10.0, DTHRON=0.0
INCON TH1ON=0.0, DTH1ON=0.0
INCON EPS20=0.0, RO=-1.0

*  CALCULATE OTHER PARAMETERS
      WN=SQRT((KTHETA*KJET)/(KF*IRIG))
      TSTAR=2.*3.14159/WN
      W1U=PHIU*WN
      THI=THIN*DB
      THRO=THRON*DB
      TH10=TH1ON*DB
      DTHRO=DTHRON*DB/TSTAR
      DTH10=DTH1ON*DB/TSTAR
      THO=THRO+TH10
      DTHO=DTHRO+DTH10

*  PUNCH CARDS OF INITIAL INFORMATION
NOSORT
      WRITE(2,10)BETA,PHIC,PHIU
   10 FORMAT(5HBETA=,F4.2,5X,5HPHIC=,E15.6,5X,5HPHIU=,E15.6)
      WRITE(2,11)DAMP,K1C,K1U,TD
   11 FORMAT(5HDAMP=,F7.5,5H K1C=,E15.6,5H K1U=,E15.6,4H TD=,E15.6)
      WRITE(2,12)THRON,DTHRON,TH1ON,DTH1ON,THIN,TSTAR
   12 FORMAT(6E12.5)
SORT

DYNAMIC

*  BODY DYNAMICS
      ALPHA=TNET/IRIG
      THR=CMPXPL(THRO,DTHRO,0.0,0.0,ALPHA)
      A=CMPXPL(TH10,DTH10,DAMP,W1U,ALPHA)
      TH1=A*K1U
      TH=THR+TH1
      DTH=DERIV(DTHO,TH)
      DTH1=DERIV(DTH10,TH1)

*  PSEUDO-RATE CONTROLLER
      EPS3=EPS1-EPS2
      R=RELAY(RO,H,EPS3)
      F=REALPL(EPS20,TAUF,R)
      EPS2=KF*F

*  OTHER BLOCKS AND VARIABLES
      THE=THI-TH
      EPS1=THE*KTHETA
      TC=KJET*R
      TNET=TC+TD
      DTON=ABS(R)
      TON=INTGRL(0.0,DTON)

*  NON-DIMENSIONALIZE OUTPUT VARIABLES
      THN=TH/DB
      DTHN=(TSTAR/DB)*DTH
      TH1N=TH1/DB
      DTH1N=(TSTAR/DB)*DTH1
      TIMEN=TIME/TSTAR
      TONN=TON/TSTAR

METHOD MILNE
ABSERR THR=0.000005,A=0.000005,F=0.000005
RELERR THR=0.000005,A=0.000005,F=0.000005
TIMER FINTIM=900., OUTDEL=1., PRDEL=1., DELMIN=1.0E-6
FINISH TIMEN=20.
PREPARE TIMEN,THN,DTHN,TH1N,DTH1N,TONN
PRINT TIMEN,THN,DTHN,TH1N,DTH1N,TONN
NOSORT
      CALL PUNCH(1)
SORT

TERMINAL

*  CODE A CARD TO TERMINATE DATA DECK
      PR=-10.
      WRITE(2,15)PR
   15 FORMAT(E13.6)
      CALL PUNCH(-1)

END
STOP
      FUNCTION RELAY(K,TIC,H,EPS3)
COMMON MEM
      EQUIVALENCE(C(1),TIME)
      I=K+KPT1-1
      T=0.
      IF(TIME)4,4,5
    4 SYMB(I)=TIC
      GO TO 50
    5 IF(EPS3 .GE. 1.)T=1.
      IF(EPS3 .LE.-1.)T=-1.
      IF((EPS3 .GT. (1.-H)) .AND. (EPS3 .LT. 1.))GO TO 15
      IF((EPS3 .LT. (-1.+H)) .AND. (EPS3 .GT. (-1.)))GO TO 20
      GO TO 40
   15 IF(ABS(SYMB(I)-1.) .LE. 0.01)T=1.
      GO TO 40
   20 IF (ABS(SYMB(I)+1.) .LE. 0.01)T=-1.
   40 SYMB(I)=T
   50 RELAY = SYMB(I)
      RETURN
      END
      SUBROUTINE PUNCH(JB)
      DIMENSION IBUF(50),XBUF(50)
      DIMENSION ITITLE(1)
      DIMENSION IBCD(2)
      REAL*8 BEGIN,XMETH,DBLANK/'
      DOUBLE PRECISION BUF(50),VAR
      DOUBLE PRECISION PNAME(100),HDNG(50),GLABEL(110),TITLE(55),TYPINT(
     $9),WORD,RERUN,ENDFIL
      COMMON DDUM1(46),TYPINT,C(8000)
      COMMON NALARM,KPOINT,KPRINT,TPRINT,KPLOT,KLAB,TPLOT,KFINIS,KRANGE,
     $KLOCK,INTYPE,KREL,KABS,KPT1,TLAST,RLAST,ALAST,KTITLE
      COMMON RMIN(100),RMAX(100),TRMIN(100),TRMAX(100)
      COMMON H,KEEP,TITLE,HDNG,INDEXP(50),IRANGE(100)
      COMMON DDUM2(20),WORD,DDUM3(105)
      COMMON TIMEX,NORES,IOPT,FR10,TNEXT,NGRAPH,KGRAPH
      COMMON DDUM4(150),INDXPP(50),PNAME,GLABEL,XOUT(50),INDEXG(50)
      COMMON IDXFAM,NFAM,KFAM,ENDS,RERUN,ENDFIL,IEND,IFIRST,IPLOT,IPRINT
     $,IFLAG(30),LINE,LINE1,IIFLAG(6)
      COMMON FAM(50),NOTING,NOSYMB,SYMB(1)
      EQUIVALENCE(C(1),TIME),(C(2),DELT),(C(3),DELMIN),(C(4),FINTIM),(C(
     $5),PRDEL),(C(6),OUTDEL)
      EQUIVALENCE(H,DELTA),(TITLE(1),ITITLE(1))
      EQUIVALENCE(BUF(1),IBUF(1)),(BUF(26),XBUF(1))
      EQUIVALENCE(BEGIN,IBCD(1)),(IIFLAG(1),IDEBUG)
      IF(JB.LT.0)GO TO 18
      IF(KEEP.NE.1)GO TO 1500
  300 DO 1200 I=1,KGRAPH
      K=INDEXG(I)
 1200 XOUT(I)=C(K)
      TN=TPLOT
      IF(ABS(XOUT(1)-TN).GT.0.00001)GO TO 1500

   13 WRITE(2,14)(XOUT(I),I=2,KGRAPH)
   14 FORMAT(6E13.6)
      GO TO 1500
   18 WRITE(2,19)(RMIN(I),I=2,KRANGE)
      WRITE(2,19)(TRMIN(I),I=2,KRANGE)
      WRITE(2,19)(RMAX(I),I=2,KRANGE)
      WRITE(2,19)(TRMAX(I),I=2,KRANGE)
   19 FORMAT(6E13.6)
 1500 RETURN
      END
ENDJOB
/*
//
******************************************************************************
      THE FOLLOWING IS PROGRAM SIGVALS,  THE CALC OF SIGNIFICANT SIMULATION
      VALUES
******************************************************************************

//  1181,FIAH,10,20,400),'MALICH',CLASS=A,MSGLEVEL=(2,0)
/*PRIORITY     4
// EXEC FORTLEGO,REGION.GO=75K
//FORT.SYSIN DD *
C
C     PROGRAM TO CALCULATE TIME IN DB ZONE   (=TINDB)
C
      DIMENSION VMIN(6), TMIN(6), VMAX(6), TMAX(6), ZMAX(6)
      NRD=5
      NPRT=6
      NPNCH=7
      WRITE(NPRT,715)
  715 FORMAT(1H1,42X,'SIGNIFICANT VALUES FROM PERFLEX DATA'//)
      WRITE(NPRT,717)
  717 FORMAT(7X,31HMAX. ABS. VAL. BEFORE TIMEN=2.0,18X,30HMAX. ABS. VAL.
     1 AFTER TIMEN=2.0,10X,7HPERCENT,7X,4HFUEL)
      WRITE(NPRT,718)
  718 FORMAT(2X,8HMIN. THN,6X,4HDTHN,7X,4HTH1N,6X,5HDTH1N,11X,3HTHN,8X,
     1  4HDTHN,7X,4HTH1N,6X,5HDTH1N,4X,10HTIME IN DB,5X,6HFACTOR//)
    3 READ(NRD,550)BETA,PHIC,PHIU
  550 FORMAT(5X,F4.2,10X,E15.6,10X,E15.6)
C***  END OF DATA SET WHEN BETA IS NEGATIVE
      IF(BETA)63,8,8
    8 READ(NRD,551)AK1U
  551 FORMAT(37X,E15.6/)
      TINDB=0.0
   10 READ(NRD,552)TIMEN,THN,DTHN,TH1N,DTH1N,TONN
  552 FORMAT(6E13.6)
      IF(ABS(THN)-1.0)15,20,20
   15 IT=0
      GO TO 25
   20 IT=1
   25 IF(TIMEN)30,50,35
   35 IF(IT-ITLST)40,50,45
   40 TSTRT=(TIMEN+TLST)/2.
      ICODE=0
      GO TO 50
   45 TEND=(TIMEN+TLST)/2.
      TINDB=TINDB+TEND-TSTRT
      ICODE=1

   50 ITLST=IT
      TLST=TIMEN
C***  SECTION A  --  FIND MAX ABS. VALUE OF VARIABLES UP TO TIMEN=2.0
      IF(TIMEN-2.)110,110,205
  110 X1=THN
      X2=ABS(DTHN)
      X3=ABS(TH1N)
      X4=ABS(DTH1N)
      IF(TIMEN)120,115,120
  115 X1MIN=0.0
      X2MAX=X2
      X3MAX=X3
      X4MAX=X4
      Y1MAX=0.0
      Y2MAX=0.0
      Y3MAX=0.0
      Y4MAX=0.0
      GO TO 190
  120 IF(X1MIN-X1)130,130,125
  125 X1MIN=X1
  130 IF(X2MAX-X2)135,140,140
  135 X2MAX=X2
  140 IF(X3MAX-X3)145,150,150
  145 X3MAX=X3
  150 IF(X4MAX-X4)155,190,190
  155 X4MAX=X4
  190 CONTINUE
C***  END OF SECTION A
C***  SECTION B  --  FIND MAX ABS. VALUE OF VARIABLES AFTER TIMEN=2.0
  205 IF(TIMEN-2.0)27,27,210
  210 Y1=ABS(THN)
      Y2=ABS(DTHN)
      Y3=ABS(TH1N)
      Y4=ABS(DTH1N)
      IF(Y1MAX-Y1)225,230,230
  225 Y1MAX=Y1
  230 IF(Y2MAX-Y2)235,240,240
  235 Y2MAX=Y2
  240 IF(Y3MAX-Y3)245,250,250
  245 Y3MAX=Y3
  250 IF(Y4MAX-Y4)255,290,290
  255 Y4MAX=Y4
  290 CONTINUE
C***  END OF SECTION B
   27 GO TO 10
   30 IF(ICODE)60,55,60
   55 TEND=TLST
      TINDB=TINDB+TEND-TSTRT
   60 READ(NRD,555)(VMIN(I),I=1,6)
      READ(NRD,555)(TMIN(I),I=1,6)
      READ(NRD,555)(VMAX(I),I=1,6)
      READ(NRD,555)(TMAX(I),I=1,6)
  555 FORMAT(6E13.6)
C
C***  SECTION C  --  USING CSMP MIN-MAX FACILITY, FIND MAX. ABS. VAL.
C     OF VARIABLES UP TO TIMEN=2.0.  IF TIMEN .GT. 2.0, USE SECTION
C     A VALUES
      TSTAR=42.7244
      IF(TMIN(2)/TSTAR-2.0)305,305,310
  305 A1MIN=VMIN(2)

      GO TO 315
  310 A1MIN=X1MIN
  315 DO 331 J=3,5
      IF(TMIN(J)/TSTAR-2.0)317,317,320
  317 ZA=ABS(VMIN(J))
      GO TO 321
  320 ZA=0.0
  321 IF(TMAX(J)/TSTAR-2.0)325,325,327
  325 ZB=ABS(VMAX(J))
      GO TO 328
  327 ZB=0.0
  328 IF(ZA-ZB)329,329,330
  329 ZMAX(J)=ZB
      GO TO 331
  330 ZMAX(J)=ZA
  331 CONTINUE
      IF(ZMAX(3)-X2MAX)335,335,337
  335 A2MAX=X2MAX
      GO TO 340
  337 A2MAX=ZMAX(3)
  340 IF(ZMAX(4)-X3MAX)345,345,347
  345 A3MAX=X3MAX
      GO TO 350
  347 A3MAX=ZMAX(4)
  350 IF(ZMAX(5)-X4MAX)355,355,357
  355 A4MAX=X4MAX
      GO TO 360
  357 A4MAX=ZMAX(5)
  360 CONTINUE
C***  END OF SECTION C
      TPCT=(TINDB/TLST)*100.0
      TONNR=0.26018
      FFACT=VMAX(6)/TONNR
      WRITE(NPRT,720)BETA,PHIC
  720 FORMAT(' (BETA=',F4.1,',PHIC=',F6.2,')')
      WRITE(NPRT,725)A1MIN,A2MAX,A3MAX,A4MAX,Y1MAX,Y2MAX,Y3MAX,
     1  Y4MAX,TPCT,FFACT
  725 FORMAT(1X,4E11.4,4X,4E11.4,4X,F5.2,4X,F9.3/)
      WRITE(NPNCH,726)BETA,PHI.,PHIU
  726 FORMAT(5HBETA=,F4.2,5X,5HPHIC=,E15.6,5X,5HPHIU=,E15.6)
      WRITE(NPNCH,727)A1MIN,A2MAX,A3MAX,A4MAX
  727 FORMAT(4E13.5)
      WRITE(NPNCH,728)Y1MAX,Y2MAX,Y3MAX,Y4MAX,TPCT,FFACT
  728 FORMAT(4E13.5,F8.3,F7.3)
      GO TO 3
   63 CALL EXIT
      END
/*
//GO.SYSIN DD *
*****     D A T A    I N    H E R E     *****
BETA=-.99                                                END OF DATA SET
/*
//
******************************************************************************
      THE FOLLOWING PROGRAM CALCULATES AND PLOTS THE PERFORMANCE QUALITY AREAS
******************************************************************************

// FOR
```

```
*IOCS(CARD,1132PRINTER,PLOTTER,KEYBOARD,TYPEWRITER)
*ONE WORD INTEGERS
*LIST SOURCE PROGRAM
C
C      PROGRAM TO PLOT PERFORMANCE QUALITY REGIONS
C      PEN AT R.H.S. AT START OF PLOT
C      PLOT CAN BE MADE OF EITHER CONSTRAINED OR UNCONSTRAINED PHI
C      INCLUDES CHANGEABLE SECTION FOR PERFORMANCE CRITERIA
C
    5 WRITE(1,540)
  540 FORMAT('CONSTRAINED PLOT  --  INPUT 1,  UNCONSTRAINED PLOT  --INPU
     1T 2')
      READ(6,541)ICODE
  541 FORMAT(I1)
C
C      DRAW PAGE BORDER
      CALL SCALF(1.0,1.0,0.0,-1.8)
      CALL FPLOT(1,0.0,0.0)
      CALL FPLOT(2,0.0,8.35)
      CALL FPLOT(0,10.85,8.35)
      CALL FPLOT(0,10.85,0.0)
      CALL FPLOT(-1,0.0,0.0)
C
C      SCALE PLOT AND DRAW AXIS
      CALL SCALF(8.0,1.6,-0.2,-2.625)
      CALL FGRID(0,0.0,-1.25,0.1,10)
      CALL FPLOT(-2,0.0,-1.25)
      DO 10 I=1,10
      AI=I
      ANUM=0.1*AI
      YPL=ALOG(ANUM)/2.302585
      CALL FPLOT(0,0.0,YPL)
      CALL POINT(0)
   10 CONTINUE
      DO 11 I=2,10
      AI=I
      ANUM=1.0*AI
      YPL=ALOG(ANUM)/2.302585
      CALL FPLOT(0,0.0,YPL)
      CALL POINT(0)
   11 CONTINUE
      DO 12 I=2,4
      AI=I
      ANUM=10.*AI
      YPL=ALOG(ANUM)/2.302585
      CALL FPLOT(0,0.0,YPL)
      CALL POINT(0)
   12 CONTINUE
C
C      ANNOTATE THE AXES
      DO 17 K=1,11
      AK=K-1
      P=AK/10.0
   15 XP=P-0.15/8.0
      YP=-1.25-0.2/1.6
      CALL FCHAR(XP,YP,0.1,0.1,0.0)
      WRITE(7,501)P
  501 FORMAT(F3.1)
   17 CONTINUE
   20 CALL FCHAR(-0.05,-1.03125,0.1,0.1,0.0)

      WRITE(7,505)
  505 FORMAT('0.1')
      CALL FCHAR(-0.05,-0.03125,0.1,0.1,0.0)
      WRITE(7,506)
  506 FORMAT('1.0')
      CALL FCHAR(-0.0625,0.96875,0.1,0.1,0.0)
      WRITE(7,507)
  507 FORMAT('10.0')
C
C      WRITE TITLES
      CALL FCHAR(-0.075,0.5,0.15,0.15,1.57074)
      IF(ICODE-1)101,101,102
  101 WRITE(7,542)
  542 FORMAT('PHIC')
      GO TO 105
  102 WRITE(7,543)
  543 FORMAT('PHIU')
  105 CALL FCHAR(0.925,-1.53125,0.15,0.15,0.0)
      WRITE(7,544)
  544 FORMAT('BETA')
      CALL FCHAR(0.1719,-2.125,0.15,0.15,0.0)
      WRITE(7,545)
  545 FORMAT('PLOT OF PERFORMANCE QUALITY REGIONS')
      CALL FPLOT(-2,0.1719,-2.5625)
      CALL FPLOT(-1,0.82813,-2.15625)
      CALL FCHAR(0.05,-1.5625,0.1,0.1,0.0)
      WRITE(7,600)
      CALL FCHAR(0.05,-1.6875,0.1,0.1,0.0)
      WRITE(7,601)
C
  550 READ(2,547)BETA,PHIC,PHIU
  547 FORMAT(5X,F4.2,10X,E15.6,10X,E15.6)
      IF(BETA)700,555,555
  555 READ(2,548)A1MIN,A2MAX,A3MAX,A4MAX
  548 FORMAT(4E13.5)
      READ(2,549)Y1MAX,Y2MAX,Y3MAX,Y4MAX,.PC.,FFAC.
  549 FORMAT(4E13.5,F8.3,F7.3)
C
C***  THE NEXT SECTION WILL CONTAIN ONE OF THE PERFORMANCE CRITERIA.
C***  QUALITY WILL BE GRADED AS A,B,C, ETC.   REGIONS ARE THEN PLOTTED
C
      XPLT=BETA-0.009375
      IF(ICODE-1)602,602,603
  602 YPLT=ALOG(PHIC)/2.302585-0.046875
      GO TO 605
  603 YPLT=ALOG(PHIU)/2.302585-0.046875
  605 CALL FCHAR(XPLT,YPLT,0.15,0.15,0.0)
C
  800 FORMAT('A')
  801 FORMAT('B')
  802 FORMAT('C')
  803 FORMAT('D')
  804 FORMAT('E')
C
*****ONE OF THE STABILITY CRITERIA GOES IN HERE   *****
C***
  700 CALL FPLOT(1,1.5,-3.125)
    6 CALL EXIT
      END
// XEQ

*****   D A T A   I N   H E R E   *****
   -.99

*****************************************************************************
   THE FOLLOWING ARE THE VARIOUS PERFORMANCE CRITERIA SECTIONS  WHICH
   ARE INSERTED INTO THE PREVIOUS PERFORMANCE REGION PROGRAM
*****************************************************************************

CRITERIA 1  --  TOTAL FUEL EXPENDED
  600 FORMAT('PERFORMANCE CRITERIA 1')
  601 FORMAT('TOTAL FUEL EXPENDED')
      IF(FFACT-1.4)615,610,610
  610 WRITE(7,611)
  611 FORMAT('D')
      GO TO 550
  615 IF(FFACT-1.2)625,620,620
  620 WRITE(7,621)
  621 FORMAT('C')
      GO TO 550
  625 IF(FFACT-1.0)635,635,630
  630 WRITE(7,631)
  631 FORMAT('B')
      GO TO 550
  635 WRITE(7,636)
  636 FORMAT('A')
      GO TO 550
C***  END OF CRITERIA 1

CRITERIA 2  --  TIME IN DEADBAND
  600 FORMAT('PERFORMANCE CRITERIA 2')
  601 FORMAT('TIME IN DEADBAND')
      IF(TPCT-85.0)615,615,610
  610 WRITE(7,611)
  611 FORMAT('A')
      GO TO 550
  615 IF(TPCT-70.0)625,625,620
  620 WRITE(7,621)
  621 FORMAT('B')
      GO TO 550
  625 IF(TPCT-55.0)635,635,630
  630 WRITE(7,631)
  631 FORMAT('C')
      GO TO 550
  635 IF(TPCT-40.0)645,645,640
  640 WRITE(7,641)
  641 FORMAT('D')
      GO TO 550
  645 WRITE(7,646)
  646 FORMAT('E')
      GO TO 550
C***  END OF CRITERIA 2

CRITERIA 3  --  INITIAL THN OVERSHOOT
  600 FORMAT('PERFORMANCE CRITERIA 3')
  601 FORMAT('INITIAL THN OVERSHOOT')

      IF(A1MIN+2.5)615,610,610
  610 WRITE(7,800)
      GO TO 550
  615 IF(A1MIN+3.0)625,620,620
  620 WRITE(7,801)
      GO TO 550
  625 IF(A1MIN+3.4165)635,630,630
  630 WRITE(7,802)
      GO TO 550
  635 WRITE(7,803)
      GO TO 550
C***  END OF CRITERIA 3

CRITERIA 4  --  INITIAL MAX DTHN
  600 FORMAT('PERFORMANCE CRITERIA 4')
  601 FORMAT('INITIAL MAX DTHN')
      IF(A2MAX-115.0)615,615,610
  610 WRITE(7,804)
      GO TO 550
  615 IF(A2MAX-100.0)625,625,620
  620 WRITE(7,803)
      GO TO 550
  625 IF(A2MAX-85.0)640,640,635
  635 WRITE(7,802)
      GO TO 550
  640 IF(A2MAX-70.0)650,650,645
  645 WRITE(7,801)
      GO TO 550
  650 WRITE(7,800)
      GO TO 550
C***  END OF CRITERIA 4

CRITERIA 5  --  INITIAL MAX TH1N
  600 FORMAT('PERFORMANCE CRITERIA 5')
  601 FORMAT('INITIAL MAX TH1N')
      IF(A3MAX-8.0)615,610,610
  610 WRITE(7,804)
      GO TO 550
  615 IF(A3MAX-6.0)625,620,620
  620 WRITE(7,803)
      GO TO 550
  625 IF(A3MAX-4.0)635,630,630
  630 WRITE(7,802)
      GO TO 550
  635 IF(A3MAX-2.0)645,640,640
  640 WRITE(7,801)
      GO TO 550
  645 WRITE(7,800)
      GO TO 550
C***  END OF CRITERIA 5

CRITERIA 6  --  INITIAL MAX DTH1N
  600 FORMAT('PERFORMANCE CRITERIA 6')
  601 FORMAT('INITIAL MAX DTH1N')
      IF(A4MAX-90.0)615,615,610
  610 WRITE(7,804)
      GO TO 550
  615 IF(A4MAX-65.0)625,625,620
  620 WRITE(7,803)
      GO TO 550
  625 IF(A4MAX-40.0)635,635,630
  630 WRITE(7,802)
      GO TO 550
  635 IF(A4MAX-15.0)645,645,640
  640 WRITE(7,801)
      GO TO 550
  645 WRITE(7,800)
      GO TO 550
C***  END OF CRITERIA 6

CRITERIA 7  --  SECONDARY MAX THN
  600 FORMAT('PERFORMANCE CRITERIA 7')
  601 FORMAT('SECONDARY MAX THN')
      IF(Y1MAX-1.45)615,615,610
  610 WRITE(7,804)
      GO TO 550
  615 IF(Y1MAX-1.35)625,625,620
  620 WRITE(7,803)
      GO TO 550
  625 IF(Y1MAX-1.25)635,635,630
  630 WRITE(7,802)
      GO TO 550
  635 IF(Y1MAX-1.15)645,645,640
  640 WRITE(7,801)
      GO TO 550
  645 WRITE(7,800)
      GO TO 550
C***  END OF CRITERIA 7

CRITERIA 8  --  SECONDARY MAX DTHN
  600 FORMAT('PERFORMANCE CRITERIA 8')
  601 FORMAT('SECONDARY MAX DTHN')
      IF(Y2MAX-10.0)615,615,610
  610 WRITE(7,804)
      GO TO 550
  615 IF(Y2MAX-7.5)625,625,620
  620 WRITE(7,803)
      GO TO 550
  625 IF(Y2MAX-5.0)635,635,630
  630 WRITE(7,802)
      GO TO 550
  635 IF(Y2MAX-2.5)645,645,640
  640 WRITE(7,801)
      GO TO 550
  645 WRITE(7,800)
      GO TO 550
C***  END OF CRITERIA 8

CRITERIA 9  --  SECONDARY MAX TH1N
  600 FORMAT('PERFORMANCE CRITERIA 9')
  601 FORMAT('SECONDARY MAX TH1N')
      IF(Y3MAX-5.0)615,615,610
  610 WRITE(7,804)
      GO TO 550

  615 IF(Y3MAX-3.5)625,625,620
  620 WRITE(7,803)
      GO TO 550
  625 IF(Y3MAX-2.0)635,635,630
  630 WRITE(7,802)
      GO TO 550
  635 IF(Y3MAX-0.5)645,645,640
  640 WRITE(7,801)
      GO TO 550
  645 WRITE(7,800)
      GO TO 550
C***  END OF CRITERIA 9

CRITERIA 10  --  SECONDARY MAX DTH1N
  600 FORMAT('PERFORMANCE CRITERIA 10')
  601 FORMAT('SECONDARY MAX DTH1N')
      IF(Y4MAX- 8.0)615,615,610
  610 WRITE(7,804)
      GO TO 550
  615 IF(Y4MAX-6.0)625,625,620
  620 WRITE(7,803)
      GO TO 550
  625 IF(Y4MAX-4.0)635,635,630
  630 WRITE(7,802)
      GO TO 550
  635 IF(Y4MAX-2.0)645,645,640
  640 WRITE(7,801)
      GO TO 550
  645 WRITE(7,800)
      GO TO 550
C***  END OF CRITERIA 10

C*** PERFORMANCE CRITERIA 11  --  ENERGY AT COMPLETION OF SIMULATION
  550 READ(2,547)BETA,PHIC,PHIU,ENRLG
  547 FORMAT(5X,F4.2,10X,E15.6,10X,E15.6,10X,F4.1)
      IF(BETA)700,555,555
C
  600 FORMAT('PERFORMANCE CRITERIA 11')
  601 FORMAT('ENERGY AT SIMULATION COMPLETION')
      VAL1=-6.0
      VAL2=-6.0
      VAL3=-6.0
      VAL4=-7.0
      IF(ENRLG-VAL1)615,615,610
  610 WRITE(7,804)
      GO TO 550
  615 IF(ENRLG-VAL2)625,625,620
  620 WRITE(7,803)
      GO TO 550
  625 IF(ENRLG-VAL3)635,635,630
  630 WRITE(7,802)
      GO TO 550
  635 IF(ENRLG-VAL4)645,645,640
  640 WRITE(7,801)
      GO TO 550
  645 WRITE(7,800)
      GO TO 550
C***  END OF CRITERIA 11
```

APPENDIX B

The total mechanical energy has kinetic and potential parts. The kinetic contribution can be written as:

$$T = \frac{1}{2} I_b \dot{\theta}^2 + \frac{1}{2} \int_a (x\dot{\theta} + \dot{y})^2 dm$$

$$= \frac{1}{2} I_b \dot{\theta}^2 + \frac{1}{2} \dot{\theta}^2 \int_a x^2 dm + \frac{1}{2} \int_a \dot{y}^2 dm + \dot{\theta} \int_a x\dot{y}\, dm \qquad \text{(B.1)}$$

where I_b is the inertia of the main body. A mass integral is taken over the flexible appendages, denoted by "a".

Now, from the formulae and notation of Ref. 10, we can expand θ and y as:

$$\theta = \Theta + \Sigma\, \theta_n q_n(t) \qquad \text{(B.2)}$$

$$y = \Sigma\, \delta_n(x) q_n(t) \qquad \text{(B.3)}$$

with

$$\int_a \delta_n(x)\delta_m(x) dm = I\, \theta_n \theta_m ; \qquad n \neq m \qquad \text{(B.4)}$$

$$\int_a \delta_n^2(x) dm = I_f \qquad \text{(B.5)}$$

$$\theta_n = - \frac{1}{I} \int x\delta_n(x) dm \qquad \text{(B.6)}$$

$$k_n = \frac{\theta_n^2}{\beta - \theta_n^2} \qquad \text{(B.7)}$$

Substitute (B.2) to (B.7) into (B.1), assuming one flexible mode. Further nondimensionalization by $1/2\ I_t\ \omega_n^2$ results with:

$$\frac{T}{\frac{1}{2} I\omega_c^2} = \left[\dot{\Theta}^2 + \sum \frac{\theta_n^2 \dot{q}_n^2}{k_n} \right] \Big/ \omega_c^2 \qquad \text{(B.8)}$$

The potential energy is composed of two parts. The first is the potential of elastic deflections. This can be written as (Ref. 10):

$$V_{el} = \frac{1}{2} \Sigma\, \omega_n^2 (I_f - I\, \theta_n^2) q_n^2$$

or:

$$\frac{V_{e\ell}}{\frac{1}{2} I \omega_c^2} = \sum \frac{\omega_n^2}{k_n \omega_c^2} \theta_n^2 q_n^2 \tag{B.9}$$

after nondimensionalizing.

A further potential term can be estimated for the satellite controller. It will exist for attitude angles beyond the deadband angle. If we define $\theta_{EXT} = \theta - DB$, we may write:

$$V_{cont} = \frac{1}{2} k \theta_{EXT}^2 \tag{B.10}$$

where

$$k = I \omega_c^2 \tag{B.11}$$

After substituting (B.11) into (B.10), we have:

$$\frac{V_{cont}}{\frac{1}{2} I \omega_c^2} = \theta_{EXT}^2 \tag{B.12}$$

The total dynamic energy is the sum of (B.8), (B.9) and (B.12) which, for one mode, is given by:

$$\frac{E}{\frac{1}{2} I \omega_c^2} = \left(\frac{\dot{\Theta}}{\omega_c} \right)^2 + \frac{(\dot{q}_1^2 + \omega_1^2 q_1^2)\theta_1^2}{\omega_c^2 k_1} + \theta_{EXT}^2 \tag{B.13}$$

UTIAS TECHNICAL NOTE NO. 199

Institute for Aerospace Studies, University of Toronto

EFFECTS OF STRUCTURAL FLEXIBILITY ON A REACTION JET SATELLITE ATTITUDE CONTROL SYSTEM

Malich, Gunter 21 pages 37 figures

1. Spacecraft Attitude Control 2. Spacecraft Structural Flexibility 3. Pseudo-rate Controller

I. Malich, Gunter II. UTIAS Technical Note No. 199

The performance of a satellite reaction jet attitude control system can be severely degraded by structural flexibility. Using a computer-modelled spacecraft with a pseudo-rate controller, a quantification of the performance loss is presented. Flexibility has been introduced into the simulation in a very general way by reducing elastic interaction to a series of modal frequency and gain parameters. The modelled system has been found to remain stable under all conditions studied, although performance may suffer various degrees of degradation.

Available copies of this report are limited. Return this card to UTIAS, if you require a copy.

UTIAS TECHNICAL NOTE NO. 199

Institute for Aerospace Studies, University of Toronto

EFFECTS OF STRUCTURAL FLEXIBILITY ON A REACTION JET SATELLITE ATTITUDE CONTROL SYSTEM

Malich, Gunter 21 pages 37 figures

1. Spacecraft Attitude Control 2. Spacecraft Structural Flexibility 3. Pseudo-rate Controller

I. Malich, Gunter II. UTIAS Technical Note No. 199

The performance of a satellite reaction jet attitude control system can be severely degraded by structural flexibility. Using a computer-modelled spacecraft with a pseudo-rate controller, a quantification of the performance loss is presented. Flexibility has been introduced into the simulation in a very general way by reducing elastic interaction to a series of modal frequency and gain parameters. The modelled system has been found to remain stable under all conditions studied, although performance may suffer various degrees of degradation.

Available copies of this report are limited. Return this card to UTIAS, if you require a copy.

UTIAS TECHNICAL NOTE NO. 199

Institute for Aerospace Studies, University of Toronto

EFFECTS OF STRUCTURAL FLEXIBILITY ON A REACTION JET SATELLITE ATTITUDE CONTROL SYSTEM

Malich, Gunter 21 pages 37 figures

1. Spacecraft Attitude Control 2. Spacecraft Structural Flexibility 3. Pseudo-rate Controller

I. Malich, Gunter II. UTIAS Technical Note No. 199

The performance of a satellite reaction jet attitude control system can be severely degraded by structural flexibility. Using a computer-modelled spacecraft with a pseudo-rate controller, a quantification of the performance loss is presented. Flexibility has been introduced into the simulation in a very general way by reducing elastic interaction to a series of modal frequency and gain parameters. The modelled system has been found to remain stable under all conditions studied, although performance may suffer various degrees of degradation.

Available copies of this report are limited. Return this card to UTIAS, if you require a copy.

UTIAS TECHNICAL NOTE NO. 199

Institute for Aerospace Studies, University of Toronto

EFFECTS OF STRUCTURAL FLEXIBILITY ON A REACTION JET SATELLITE ATTITUDE CONTROL SYSTEM

Malich, Gunter 21 pages 37 figures

1. Spacecraft Attitude Control 2. Spacecraft Structural Flexibility 3. Pseudo-rate Controller

I. Malich, Gunter II. UTIAS Technical Note No. 199

The performance of a satellite reaction jet attitude control system can be severely degraded by structural flexibility. Using a computer-modelled spacecraft with a pseudo-rate controller, a quantification of the performance loss is presented. Flexibility has been introduced into the simulation in a very general way by reducing elastic interaction to a series of modal frequency and gain parameters. The modelled system has been found to remain stable under all conditions studied, although performance may suffer various degrees of degradation.

Available copies of this report are limited. Return this card to UTIAS, if you require a copy.